



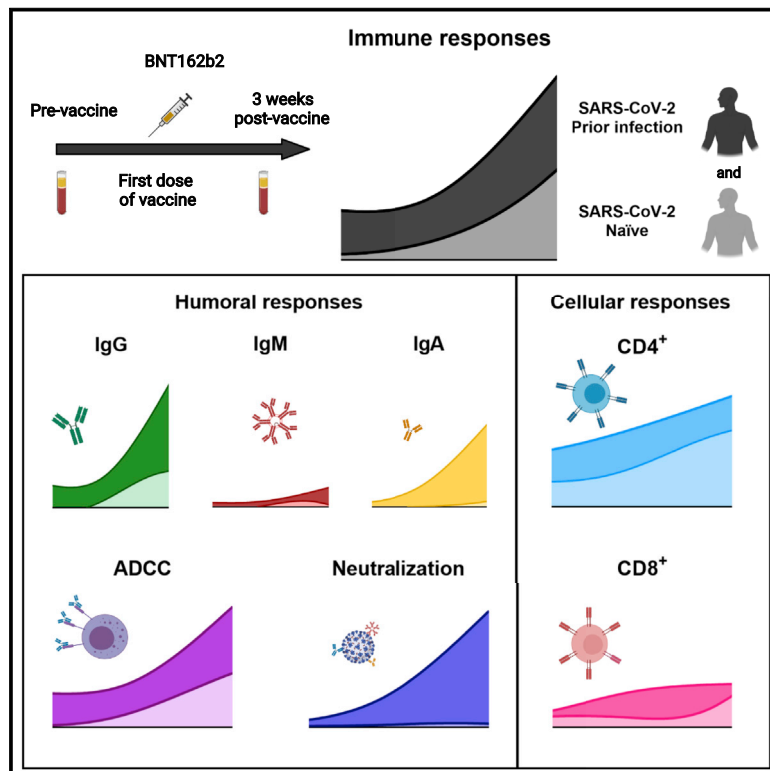
Since January 2020 Elsevier has created a COVID-19 resource centre with free information in English and Mandarin on the novel coronavirus COVID-19. The COVID-19 resource centre is hosted on Elsevier Connect, the company's public news and information website.

Elsevier hereby grants permission to make all its COVID-19-related research that is available on the COVID-19 resource centre - including this research content - immediately available in PubMed Central and other publicly funded repositories, such as the WHO COVID database with rights for unrestricted research re-use and analyses in any form or by any means with acknowledgement of the original source. These permissions are granted for free by Elsevier for as long as the COVID-19 resource centre remains active.

Cell Host & Microbe

A single dose of the SARS-CoV-2 vaccine BNT162b2 elicits Fc-mediated antibody effector functions and T cell responses

Graphical abstract



Authors

Alexandra Tauzin, Manon Nayrac, Mehdi Benlarbi, ..., Cécile Tremblay, Daniel E. Kaufmann, Andrés Finzi

Correspondence

c.tremblay@umontreal.ca (C.T.), daniel.kaufmann@umontreal.ca (D.E.K.), andres.finzi@umontreal.ca (A.F.)

In brief

Tauzin and Nayrac et al. characterize humoral and cellular responses 3 weeks after a single dose of mRNA BNT162b2 vaccine. They show, in SARS-CoV-2-naive individuals, that the antibodies elicited have weak neutralizing activity but potent Fc-mediated effector functions, and in SARS-CoV-2 previously infected individuals, that all responses are significantly boosted.

Highlights

- Three weeks after the first BNT162b2 dose, weak neutralizing antibodies are elicited
- These antibodies have robust Fc-mediated effector functions
- Vaccination of individuals previously infected boosts humoral and cellular responses
- Strong correlations between T helper cell and humoral responses are observed



Article

A single dose of the SARS-CoV-2 vaccine BNT162b2 elicits Fc-mediated antibody effector functions and T cell responses

Alexandra Tauzin,^{1,2,14} Manon Nayrac,^{1,2,14} Mehdi Benlarbi,¹ Shang Yu Gong,^{1,3} Romain Gasser,^{1,2} Guillaume Beaudoin-Bussi eres,^{1,2} Nathalie Brassard,¹ Annemarie Laumaea,^{1,2} Dani V ezina,^{1,2} J er emie Pr evost,^{1,2} Sai Priya Anand,^{1,3} Catherine Bourassa,¹ Gabrielle Gendron-Lepage,¹ Halima Medjahed,¹ Guillaume Goyette,¹ Julia Niessi,^{1,2,12,13} Olivier Tastet,¹ Laurie Gokool,¹ Chantal Morrisseau,¹ Pascale Arlotto,¹ Leonidas Stamatatos,^{4,5} Andrew T. McGuire,⁴ Catherine Larochelle,^{1,6} Pradeep Uchil,⁷ Maolin Lu,⁷ Walther Mothes,⁷ Gaston De Serres,⁸ Sandrine Moreira,⁹ Michel Roger,^{1,2,9} Jonathan Richard,^{1,2} Val erie Martel-Laf erri ere,^{1,2} Ralf Duerr,¹⁰ C ecile Tremblay,^{1,2,*} Daniel E. Kaufmann,^{1,11,12,*} and Andr es Finzi^{1,2,3,15,*}

¹Centre de Recherche du CHUM, Montr al, QC H2X 0A9, Canada

²D epartement de Microbiologie, Infectiologie et Immunologie, Universit  de Montr al, Montreal, QC H2X 0A9, Canada

³Department of Microbiology and Immunology, McGill University, Montreal, QC H3A 2BA, Canada

⁴Fred Hutchinson Cancer Research Center, Vaccine and Infectious Disease Division, Seattle, WA 98109, USA

⁵University of Washington, Department of Global Health, Seattle, WA 98109, USA

⁶D epartement des Neurosciences, Universit  de Montr al, Montreal, QC H3C 3J7, Canada

⁷Department of Microbial Pathogenesis, Yale University School of Medicine, New Haven, CT 06510, USA

⁸Institut National de Sant  Publique du Qu bec, Quebec, QC, H2P 1E2, Canada

⁹Laboratoire de Sant  Publique du Qu bec, Institut National de Sant  Publique du Qu bec, Sainte-Anne-de-Bellevue, QC H9X 3R5, Canada

¹⁰Department of Microbiology, New York University School of Medicine, New York, NY 10016, USA

¹¹D epartement de M decine, Universit  de Montr al, Montreal, QC H3T 1J4, Canada

¹²Consortium for HIV/AIDS Vaccine Development (CHAVID), La Jolla, CA, USA

¹³Present address: Center for Infectious Medicine, Department of Medicine Huddinge, Karolinska Institutet, Stockholm 171 77, Sweden

¹⁴These authors contributed equally

¹⁵Lead contact

*Correspondence: c.tremblay@umontreal.ca (C.T.), daniel.kaufmann@umontreal.ca (D.E.K.), andres.finzi@umontreal.ca (A.F.)

<https://doi.org/10.1016/j.chom.2021.06.001>

SUMMARY

While the standard regimen of the BNT162b2 mRNA vaccine for SARS-CoV-2 includes two doses administered 3 weeks apart, some public health authorities are spacing these doses, raising concerns about efficacy. However, data indicate that a single dose can be up to 90% effective starting 14 days post-administration. To assess the mechanisms contributing to protection, we analyzed humoral and T cell responses three weeks after a single BNT162b2 dose. We observed weak neutralizing activity elicited in SARS-CoV-2 naive individuals but strong anti-receptor binding domain and spike antibodies with Fc-mediated effector functions and cellular CD4⁺ T cell responses. In previously infected individuals, a single dose boosted all humoral and T cell responses, with strong correlations between T helper and antibody immunity. Our results highlight the potential role of Fc-mediated effector functions and T cell responses in vaccine efficacy. They also provide support for spacing doses to vaccinate more individuals in conditions of vaccine scarcity.

INTRODUCTION

The severe acute respiratory syndrome coronavirus 2 (SARS-CoV-2) is the etiological agent of the coronavirus disease 2019 (COVID-19), responsible for the current pandemic that infected over 174 million people and led to more than 3.74 million deaths worldwide (Dong et al., 2020; World Health Organization). This pandemic caused a race for the elaboration of an effective vaccine against SARS-CoV-2 (Krammer, 2020; Moore and Klasse, 2020). Currently approved vaccines target the highly immunogenic trimeric spike (S) glycoprotein that facilitates SARS-CoV-2 entry into host cells via its receptor-binding domain (RBD),

which interacts with angiotensin-converting enzyme 2 (ACE-2) (Hoffmann et al., 2020; Walls et al., 2020). Among these vaccines, four are approved in many countries (Pfizer/BioNtech BNT162b2, Moderna mRNA-1273, AstraZeneca ChAdOx1, and Janssen Ad26.COV2S). The Pfizer/BioNtech BNT162b2 vaccine was developed using a novel technology based on mRNA (Polack et al., 2020). This technology consists of intramuscular injection of a lipid nanoparticle-encapsulated synthetic mRNA vaccine encoding the viral S glycoproteins of SARS-CoV-2, which has shown to elicit a robust efficacy against the Wuhan-Hu-1 strain, which served as template for their development (Baden et al., 2021; Sahin et al., 2020a). This vaccine encodes



Table 1. Characteristics of the vaccinated SARS-CoV-2 cohort

Group	n	Days between symptom onset and vaccination (median; day range)	Days after vaccination (median; day range)	Age (average; age range)	Gender	
					F (n)	M (n)
SARS-CoV-2 naive	24	/	21 (16 - 28)	46 (21-59)	17	7
SARS-CoV-2 prior infection	24	279 (61-326)	21 (13 - 26)	47 (23-65)	14	10

for a membrane-anchored SARS-CoV-2 full-length S, stabilized in a prefusion conformation by mutating the furin cleavage site and introducing two prolines in the S2 fusion machinery (Polack et al., 2020; Wrapp et al., 2020). However, the emergence of mutations in the SARS-CoV-2 S glycoprotein could affect different properties of the virus including affinity for its receptor, resulting in increased infectivity, transmissibility, and evasion from humoral responses elicited by natural infection or vaccination (Prévost and Finzi, 2021).

The D614G S mutation appeared very early in the pandemic and is now highly prevalent in all circulating strains (Isabel et al., 2020). The B.1.1.7 variant was first identified in the United Kingdom and has been spread rapidly to many countries since its identification. This variant contains several mutations in its S glycoprotein (Δ H69-V70, Δ Y144, N501Y, A570D, P681H, T716I, S982A, and D1118H) and has increased infectivity (Davies et al., 2020; Rambaut et al., 2020). Among the mutations present in the B.1.1.7 strain, the N501Y is also present in many other circulating variants (B.1.351 and P.1) and increases the affinity for the ACE-2 receptor (Chan et al., 2020b; Corum and Zimmer, 2021). The E484K mutation is part of the South African B.1.351 variant and is now found in several SARS-CoV-2 genomes worldwide that spread rapidly (Gröhs Ferrareze et al., 2021). Studies have shown that this mutation increases affinity of the S glycoprotein for ACE-2 (Nelson et al., 2021) and confers resistance to neutralization mediated by monoclonal antibodies (mAbs) and plasma from naturally infected and vaccinated individuals (Ku et al., 2021; Stamatatos et al., 2021; Tada et al., 2021; Wang et al., 2021). The S477N mutation confers a higher affinity for the ACE-2 receptor and has rapidly spread to many countries in Oceania and Europe (Flores-Alanis et al., 2021; Hodcroft et al., 2020; Jolly et al., 2021; Mejdani et al., 2021; West et al., 2021; Wu et al., 2021). The S477N and N501S mutations are found in several SARS-CoV-2 genomes in Quebec (S.M. and M.R., unpublished data).

In spite of the proven clinical efficacy of BNT162b2, there are still limitations in the understanding of the protective components of the immune responses elicited by this vaccine. Such protection is mediated through a complex interplay between innate, humoral, and cell-mediated immunity (Pulendran and Ahmed, 2011; Sallusto et al., 2010). Several reports showed that administration of the mRNA vaccine induced a strong humoral response after two doses, especially against the RBD domain (Ju et al., 2020; Wu et al., 2020). Robust CD4⁺ and CD8⁺ memory T cell responses are induced after SARS-CoV-2 infection (Breton et al., 2021; Dan et al., 2021) and play important roles in resolution of the infection (Sette and Crotty, 2021) including modulating disease severity in humans (Rydzynski Moderbacher et al., 2020) and reducing viral load in non-human primates (NHPs) (Muñoz-Fontela et al., 2020). However, the

detection of these specific memory T cells has been poorly studied in the SARS-CoV-2 vaccine development and represents a gap in the understanding of the induced cellular adaptive immune responses, which are likely to also play an important role (Sahin et al., 2020a). Among CD4⁺ T cells, the T follicular helper (Tfh) subset is of particular interest, as it provides help for B cell maturation and development of high-affinity antibody (Ab) responses in the germinal center (GC) of secondary lymphoid organs. Studies have shown that a subset of CXCR5⁺ in blood, called circulating Tfh (cTfh) (Crotty, 2014; Morita et al., 2011), has clonal, phenotypic, and functional overlap with GC Tfh and reflects, at least in part, responses in tissues (Heit et al., 2017; Vella et al., 2019).

Results from phase III clinical trials have shown a vaccine efficacy of >90% starting 14 days after the injection of a single dose of BNT162b2 mRNA vaccine, thus before the administration of a second dose (Baden et al., 2021; Polack et al., 2020; Skowronski et al., 2021). In this report, we characterized the humoral and T cell immune responses in cohorts of SARS-CoV-2 naive and naturally infected individuals prior and 3 weeks after a first dose of the BNT162b2 mRNA vaccine.

RESULTS

Here, we analyzed humoral and cellular responses in blood samples from 24 SARS-CoV-2 naive donors prior and after vaccination (median [range]: 21 days [16–28 days]). In addition, we examined the same immunological features in 24 individuals that were previously infected (PI) around 9 months before vaccination (median [range]: 279 days [61–326 days]) and 3 weeks after vaccination (median [range]: 21 days [13–26 days]). For 16 of these donors, we also longitudinally monitored evolution of the humoral response, from 6 weeks post-symptom onset (PSO, median [range]: 44 days [16–95 days]) to 3 weeks after vaccination. Basic demographic characteristics are summarized in Table 1. In the SARS-CoV-2 naive group, the average age of donors was 46 years (range: 21–59 years), and samples were from 7 males and 17 females. In the group of PI individuals, the average age of the donors was 47 years (range: 23–65 years), and samples were from 10 males and 14 females (Table 1).

Elicitation of SARS-CoV-2 antibodies against the full spike and its receptor-binding domain

To evaluate vaccine responses in SARS-CoV-2 naive and PI individuals, we first measured the presence of RBD-specific Abs (IgG, IgM, and IgA) using a previously described enzyme-linked immunosorbent (ELISA) RBD assay (Beaudoin-Bussièrès et al., 2020; Gasser et al., 2021; Prévost et al., 2020). As expected, in the SARS-CoV-2 naive group, we did not observe RBD-specific immunoglobulins (Ig) in samples recovered before vaccination

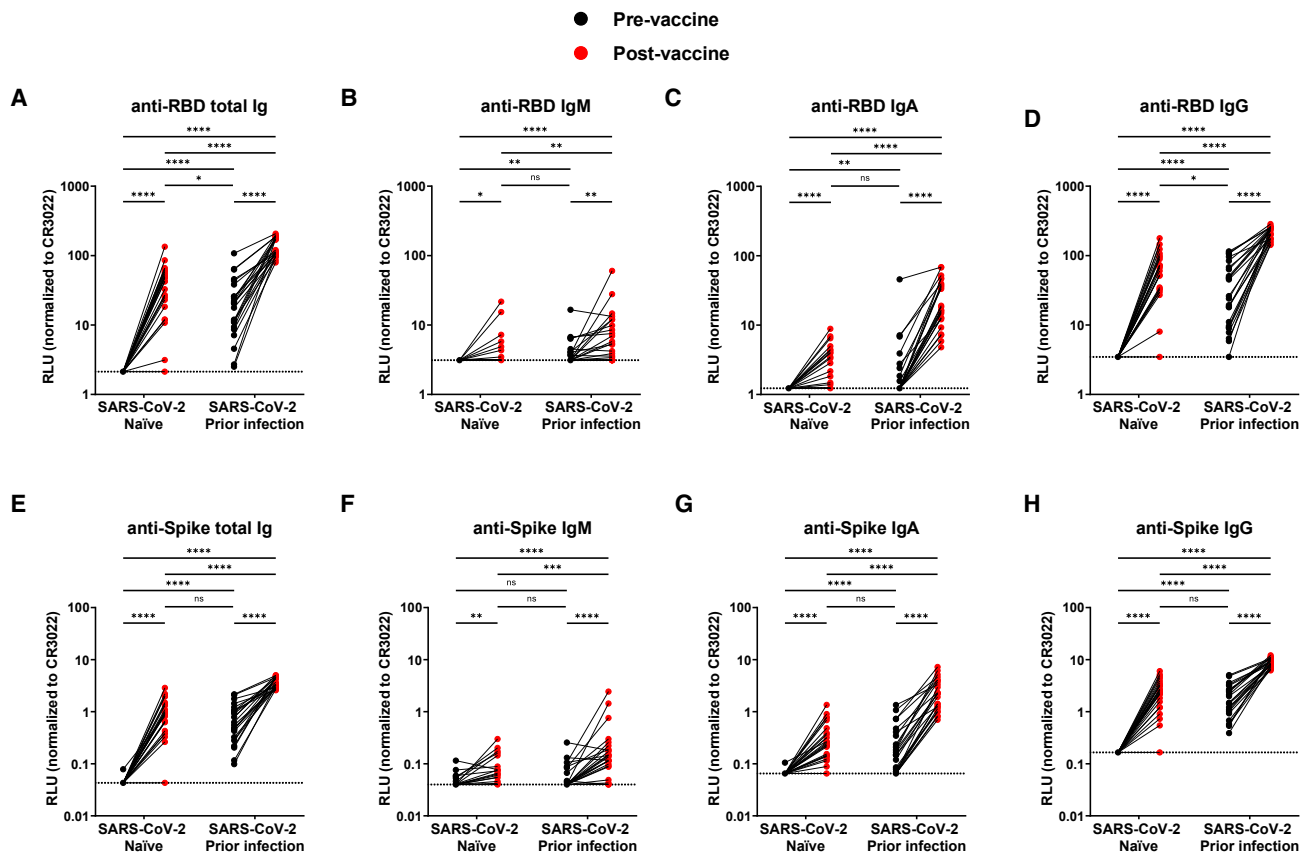


Figure 1. Elicitation of RBD- and spike-specific antibodies by a single dose of Pfizer/BioNTech mRNA vaccine in SARS-CoV-2 naive and previously infected individuals

(A–D) Indirect ELISA was performed by incubating plasma samples from naive and PI donors collected before and after the first dose of vaccine with recombinant SARS-CoV-2 RBD protein. Anti-RBD Ab binding was detected using HRP-conjugated (A) anti-human IgM+IgG+IgA, (B) anti-human IgM, (C) anti-human IgA, or (D) anti-human IgG. Relative light unit (RLU) values obtained with BSA (negative control) were subtracted and further normalized to the signal obtained with the anti-RBD CR3022 mAb present in each plate.

(E–H) Cell-based ELISA was performed by incubating plasma samples from naive and PI donors collected before and after the first dose of vaccination with HOS cells expressing full-length SARS-CoV-2 S. Anti-S Ab binding was detected using HRP-conjugated (E) anti-human IgM+IgG+IgA, (F) anti-human IgM, (G) anti-human IgA, or (H) anti-human IgG. RLU values obtained with parental HOS (negative control) were subtracted and further normalized to the signal obtained with the CR3022 mAb present in each plate.

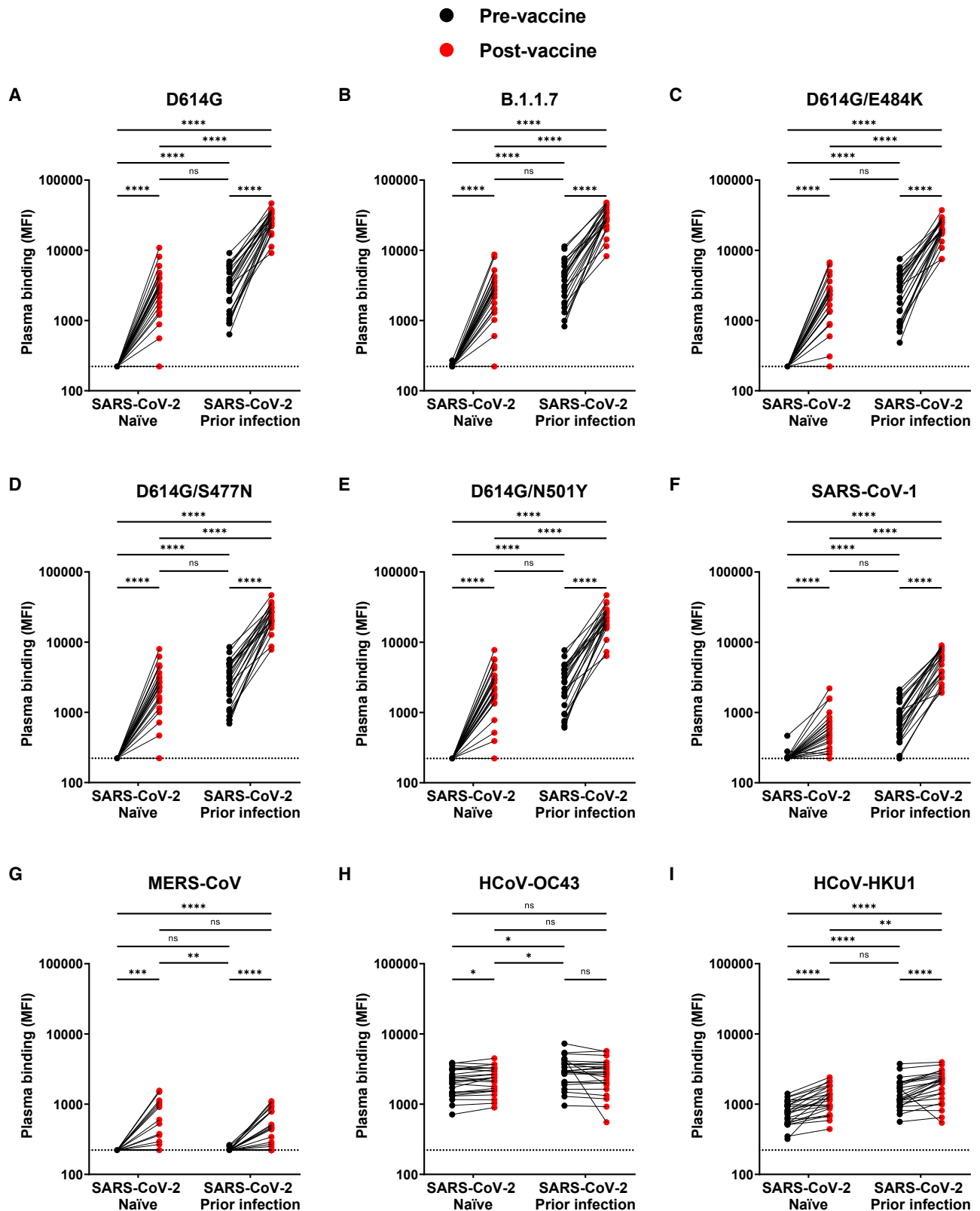
Limits of detection are plotted (* $p < 0.05$; ** $p < 0.01$; *** $p < 0.001$; **** $p < 0.0001$; ns, non-significant).

(Figures 1A–1D). Three weeks after the first dose, we found a significant increase in the total RBD-specific Ig levels with the exception of one donor from the naive group who didn't respond to the vaccine at this time point. Vaccination induced similar levels of IgM and IgA targeting the RBD to those present in individuals that were naturally infected 9 months before (Figures 1B and 1C). In addition, RBD-specific IgG levels were significantly higher in the vaccinated SARS-CoV-2 naive group compared to pre-vaccination samples from the PI participants (Figure 1D).

In the group of individuals that were PI, despite a decline in the amount of anti-RBD-specific antibodies over time after infection (Figures S1A–S1D), most donors still had detectable anti-RBD-specific Abs just before vaccination, especially anti-RBD IgG (Figures 1A–1D). For all participants, the first dose of vaccination led to a robust increase in anti-RBD IgG and anti-RBD IgA levels, higher than the first time point measured PSO (16–95 days; median: 44 days) (Figures 1C–1D and S1C–S1D). Vaccination

modestly increased the level of RBD-specific IgM (Figures 1B and S1B). Among the studied humoral responses, anti-SARS-CoV-2 neutralization returned to baseline most promptly, whereas antibody-dependent cellular cytotoxicity (ADCC) remained more robust in the convalescent stage while still responding with a significant increase post-vaccination (Figures S1E–S1G).

To evaluate whether vaccine responses were limited to RBD or could be extended to Abs against the full S glycoprotein, we used a cell-based ELISA (CBE) assay to measure levels of Abs recognizing the native full-length S glycoprotein expressed at the cell surface (Anand et al., 2021b). In SARS-CoV-2 naive individuals, the pattern was similar to that observed for the anti-RBD specific response, with a level of total S-specific Ig similar to that observed in PI individuals before vaccination (Figure 1E). As we observed for anti-RBD Abs, vaccination of naive individuals elicited higher levels of IgG than IgM or IgA (Figures 1F–1H).



(legend on next page)

The individual who did not elicit anti-RBD Abs upon vaccination didn't elicit Abs against other regions of the S, with detection levels no higher than our seropositivity threshold level (Figures 1E–1H).

Thus, vaccination in the SARS-CoV-2 naive group elicited Abs against the RBD and full S that reached similar levels than in naturally infected individuals 9 months PSO (Figure 1).

Recognition of SARS-CoV-2 spike variants and other Betacoronaviruses

SARS-CoV-2 is evolving, and variants of concern are emerging globally. Some harbor specific mutations in S that are associated with increased transmissibility and/or immune evasion (Davies et al., 2020; Sabino et al., 2021; Tegally et al., 2020; Volz et al., 2021). To evaluate whether a single dose of the Pfizer/BioNTech vaccine elicits Abs that are able to recognize a broader spectrum of variants, including S with putative escape mutations, we measured the ability of plasma from vaccinated individuals to recognize different S variants expressed at the cell surface by flow cytometry, using a method we recently reported (Prévost et al., 2020). As expected, none of the SARS-CoV-2 naive plasma samples obtained before vaccination (baseline) recognized the SARS-CoV-2 S (D614G) or any of its variants (Figures 2A–2E). However, they were able to recognize S from endemic human coronaviruses (HCoV-OC43 and HCoV-HKU1) but not S from highly pathogenic coronaviruses (SARS-CoV-1 and MERS-CoV) (Figures 2F–2I). In agreement with our CBE results (Figure 1), vaccination elicited Abs that efficiently recognized the full S and all the tested variants (Figures 2A–2E), except for the same donor that did not elicit RBD- or S-specific Abs. The recognition levels were equivalent to those observed for PI individuals before vaccination. In the latter group, all plasma samples recognized the different S variants before vaccination, and the first dose of vaccine led to a significant increase in S recognition (Figures 2A–2E). When we compared the differences in recognition between the SARS-CoV-2 variants, we observed that plasma from vaccinated naive individuals recognized the different SARS-CoV-2 variants less efficiently compared to D614G S (Figure S2A). Plasma from PI individuals recognized all SARS-CoV-2 S before and after vaccination (Figures S2B and S2C). Vaccination, however, robustly enhanced recognition in this group, albeit a bit less efficiently for the S variants (Figure S2C).

We recently reported that SARS-CoV-2 infection elicits cross-reactive Abs that can recognize S from other human coronaviruses (Beaudoin-Bussi eres et al., 2020; Pr evost et al., 2020). To evaluate whether vaccination also elicited Abs able to recognize S glycoproteins from other *Betacoronaviruses*, we evaluated the capacity of the different plasma samples to bind cell-surface-expressed S from SARS-CoV-1, MERS-CoV, HCoV-OC43, and HCoV-HKU1. As shown in Figure 2 (2F–2I), vaccination elicited cross-reactive Abs in both groups with enhanced recognition of SARS-CoV-1, MERS-CoV, HCoV-HKU1, and HCoV-OC43 only in the SARS-CoV-2 naive group.

Functional activities of vaccine-elicited antibodies

A single dose of the Pfizer/BioNTech vaccine was shown to be up to 90% efficacious starting 2 weeks after administration (Skowronski and De Serres, 2021; Skowronski et al., 2021; Polack et al., 2020). Among the immune responses elicited by the different SARS-CoV-2 vaccines, the neutralizing response is thought to be associated with vaccine efficacy (Jackson et al., 2020; Muruato et al., 2020; Polack et al., 2020). To evaluate whether neutralizing responses were elicited within the first 3 weeks upon vaccine administration, we measured the capacity of plasma samples to neutralize pseudoviral particles carrying the SARS-CoV-2 S glycoprotein. All pseudovirus variants were infectious in this system with SARS-CoV-2 variants, with B.1.1.7 in particular exhibiting enhanced infectivity (Figure S2D). We observed very low neutralizing activity in plasma from vaccinated naive individuals (Figure 3A), in agreement with previous findings (Collier et al., 2021; Ellebedy et al., 2021; Goel et al., 2021; Planas et al., 2021; Sahin et al., 2020b). As recently described (Krammer et al., 2021; Stamataatos et al., 2021), we observed that pre-existing SARS-CoV-2 neutralizing Ab responses were significantly boosted by a single dose of S-encoded mRNA vaccine (Figure 3A). Interestingly, a single dose enlarged the potency of the neutralizing response that was now able to efficiently neutralize pseudoviral particles bearing the B.1.1.7 S or from other variants with different concerning mutations (E484K, S477N, N501Y, and N501S) (Figures S2E–S2G). Remarkably it also boosted neutralization activity against pseudoparticles bearing the SARS-CoV-1 S (Figure S2H).

Since weak neutralizing activity was detected in SARS-CoV-2 naive vaccinated individuals, we decided to measure Fc-mediated effector functions that were also shown to play an important role against SARS-CoV-2 infection (Chan et al., 2020a; Sch afer et al., 2021; Zohar et al., 2020). In agreement with the lack of S-specific Abs, SARS-CoV-2 naive individuals did not have detectable ADCC activity prior to vaccination (Figure 3B). The first dose of the vaccine induced a significant increase in ADCC activity, except for one sample, corresponding to the donor who had not developed anti-S Abs. We noted that ADCC activity in vaccinated naive individuals achieved comparable levels to those of PI individuals before vaccination. Vaccination of this group significantly boosted the ADCC activity (Figure 3B). Based on these results, it is tempting to speculate that the generation of Abs with Fc-mediated effector functions, but with low neutralizing activity, might be sufficient to provide a certain level of protection.

Spike-specific T cell vaccine responses differ between SARS-CoV-2 naive and previously infected individuals

We examined whether prior SARS-CoV-2 infection alters the CD4⁺ and CD8⁺ T cell responses to vaccination. To measure SARS-CoV-2-S-specific T cells in the two cohorts of naive persons and PI individuals, we utilized two complementary methodologies, T cell receptor (TCR)-dependent activation-induced marker (AIM) assays and intracellular cytokine staining (ICS).

Figure 2. Detection of SARS-CoV-2 spike variants and other Betacoronaviruses

(A–I) Cell-surface staining of 293T cells expressing full-length S from different SARS-CoV-2 variants and other human *Betacoronavirus* using plasma samples collected before and after first dose of vaccination in SARS-CoV-2 naive and PI donors. The graphs represent the median fluorescence intensities (MFIs) obtained. Limits of detection are plotted (*p < 0.05; **p < 0.01; ***p < 0.001; ****p < 0.0001; ns, non-significant).

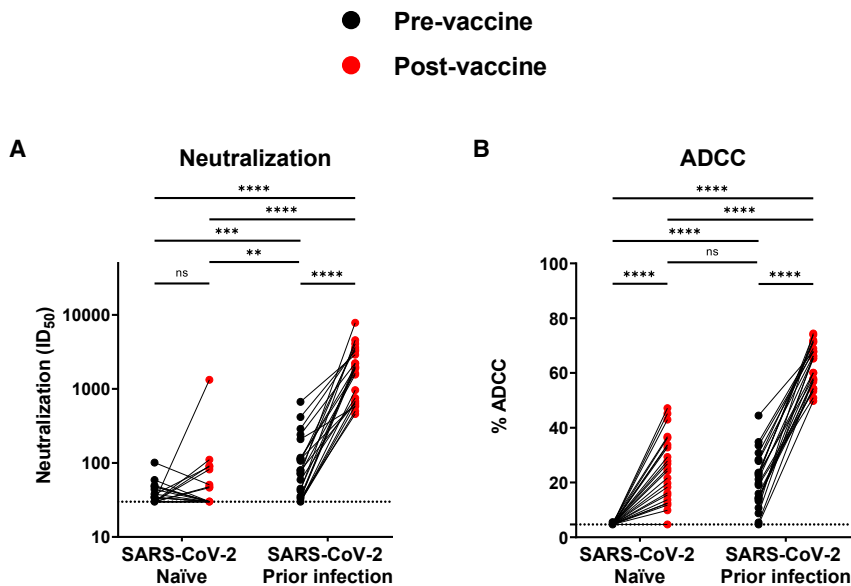


Figure 3. Neutralization and Fc-effector function activities in SARS-CoV-2 naive and previously infected individuals before and after a single dose of Pfizer/BioNTech mRNA vaccine

(A) Neutralizing activity was measured by incubating pseudoviruses bearing SARS-CoV-2 S glycoproteins, with serial dilutions of plasma for 1 h at 37°C before infecting 293T-ACE2 cells. Neutralization half maximal inhibitory serum dilution (ID_{50}) values were determined using a normalized non-linear regression using GraphPad Prism software.

(B) CEM.NKr parental cells were mixed at a 1:1 ratio with CEM.NKr-S cells and were used as target cells. PBMCs from uninfected donors were used as effector cells in a FACS-based ADCC assay. Limits of detection are plotted (** $p < 0.01$; *** $p < 0.001$; **** $p < 0.0001$; ns, non-significant).

We performed the cytokine-independent AIM assays as previously described (Reiss et al., 2017), with some modifications. We stimulated PBMC for 15 h with an overlapping peptide pool spanning the S coding sequence and measured upregulation of the markers CD69, CD40L, 4-1BB, and OX-40 upon stimulation. We used an AND/OR Boolean combination gating strategy to identify antigen-specific T cell responses (Figure S3A) (Niessl et al., 2020a). We examined three populations of SARS-CoV-2-S-specific AIM⁺ T cells: (1) AIM⁺ total CD4⁺ T cells (Figure 4A), (2) AIM⁺ cTfh cells (Figure 4B), and (3) AIM⁺ total CD8⁺ T cells (Figure 4C). We and others have shown that AIM assays can sensitively detect infection- and vaccine-induced cTfh responses (Dan et al., 2016; Niessl et al., 2020b), including in SARS-CoV-2 infection (Dan et al., 2021).

After vaccination, we observed a significant increase in total S-specific AIM⁺CD4⁺ T cell responses in both groups of participants (Figure 4A). We observed similar patterns with S-specific AIM⁺ cTfh and S-specific AIM⁺ CD8⁺ T cell responses, which significantly increased after vaccination in both groups (Figures 4B and 4C) and stronger in the PI group compared to the naive group. However, the frequencies range of the AIM⁺ CD8⁺ responses remain significantly lower than that of AIM⁺ CD4⁺ T cell responses, regardless of the time point studied (Figure S3C).

To assess functionality and polarization of the SARS-CoV-2-S-specific T cell responses, we measured by ICS the cytokines secreted by CD4⁺ and CD8⁺ T cells in response to a 6-h stimulation of PBMC with a S peptide pool. T cells were analyzed for expression of CD40L, CD107a, interferon (IFN)- γ , interleukin (IL)-2, IL-10, IL-17A, and tumor necrosis factor (TNF)- α . IL-17A expression was undetectable for most participants in both CD4⁺ and CD8⁺ T cell subsets, and CD40L negligible in CD8⁺ T cells. These subsets were thus not pursued, whereas all other functions were included in further analysis. We defined frequencies of cytokine⁺ CD4⁺ and CD8⁺ T cells as percentage of cells positive for one or more cytokines or functional markers (Figure S3B). Consistent with previous results on T cell re-

sponses specific for other viruses after natural infection (Niessl et al., 2020b; Reiss et al., 2017), the magnitude of ICS⁺ T cells was lower than that of AIM⁺ T cell responses (Figures S3D and S3E), but there was a good correlation between both assays (Figure S3F). After vaccination, the ICS⁺ CD4⁺ T cell responses were significantly increased in the two groups (Figure 4D) with stronger responses in PI group compared to the naive group. ICS⁺ CD8⁺ T cell responses were also significantly increased in PI individuals (Figure 4E); however, there were only trends for an increase after this single dose of vaccine in the naive cohort.

To qualitatively assess S-specific T cells in naive and PI groups for polyfunctional responses after vaccination, we performed co-expression analysis using Boolean gating and examined each combination of function (Figures 4F and 4G). In comparison to naive individuals, dominant S-specific CD4⁺ T subsets that were preferentially increased by vaccination in PI included S-specific CD4⁺ T cells coexpressing CD40L, or IFN- γ alone or in combination with other functions (TNF- α , CD107a, IL-2). The frequency of S-specific CD8⁺ T cells expressing IFN- γ alone or combined with CD107a was also increased in PI compared to naive participants.

These data show that while a single dose of mRNA vaccine could induce detectable S-specific CD4⁺ and CD8⁺ T cells in most individuals, including S-specific cTfh cells, independently of prior SARS-CoV-2 infection status, immunization elicited more robust and functionally skewed responses in participants with a history of SARS-CoV-2 infection, compared to naive people, with preferential expansion of specific functional subsets.

Relationship between SARS-CoV-2-spike-specific T cell responses and humoral responses

Most protective Ab responses are dependent on CD4⁺ T cell help, which is critical for B cell expansion, affinity maturation, and isotype switching. Therefore, we assessed whether pre-existing SARS-CoV-2-S-specific CD4⁺ T cells and cTfh responses were predictive of higher Ab titers and Ab functions, as measured by neutralization capacity and ADCC after vaccination, irrespective of prior infection status (Figure 5A). We found that correlations between the function-agnostic AIM⁺ CD4⁺

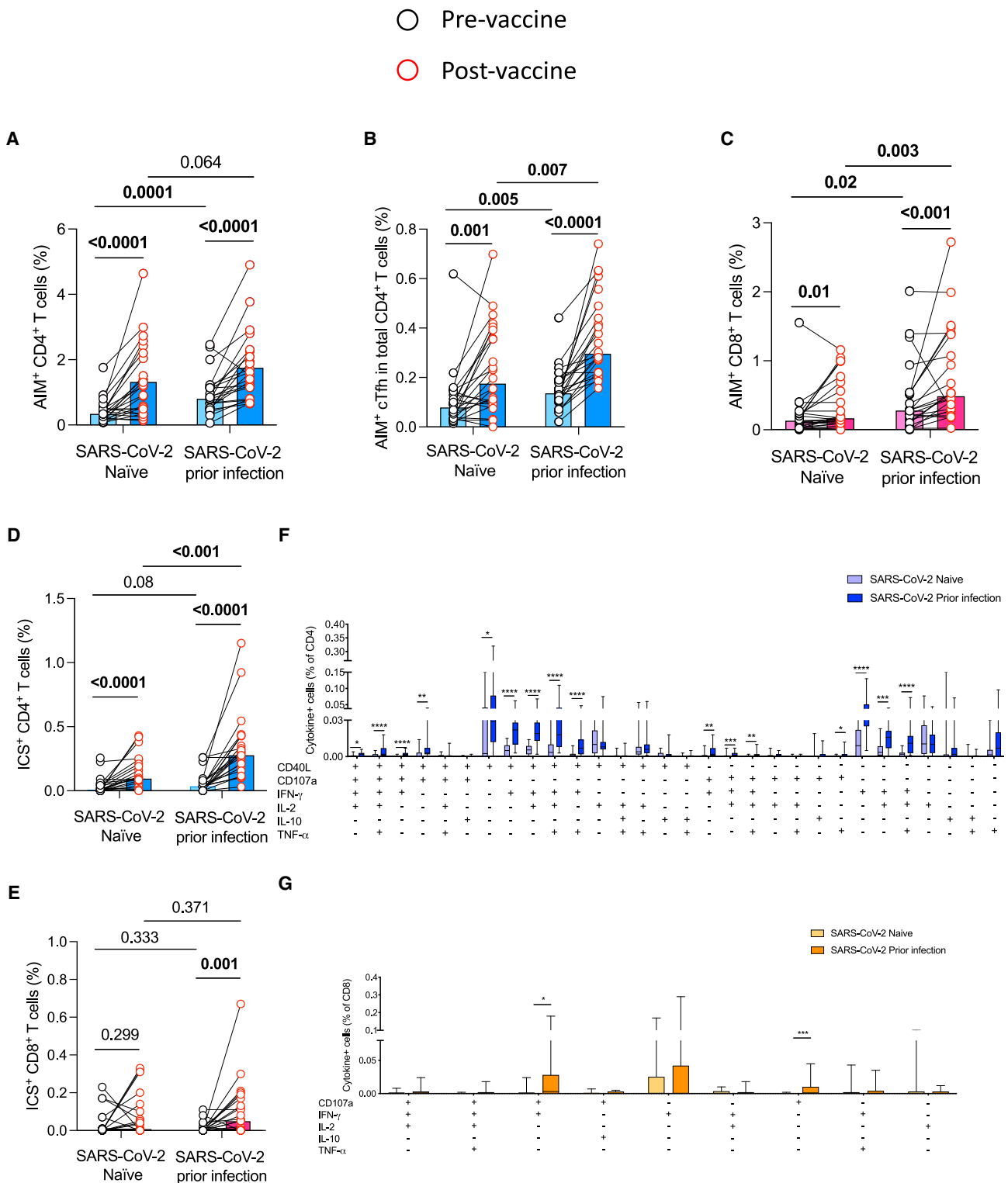


Figure 4. Spike-specific CD4⁺ and CD8⁺ T cell vaccine responses quantitatively and qualitatively differ in SARS-CoV-2 naive versus previously infected individuals

(A–C) Net frequencies after S peptide pool stimulation of (A) total S-specific AIM⁺ CD4⁺ T cells, (B) S-specific AIM⁺ cTfh, (C) S-specific AIM⁺ CD8⁺ T cells in each donor prior to (V0) and post- (V1) vaccination in the SARS-CoV-2 naive participants and those with previous SARS-CoV-2 infection.

(legend continued on next page)

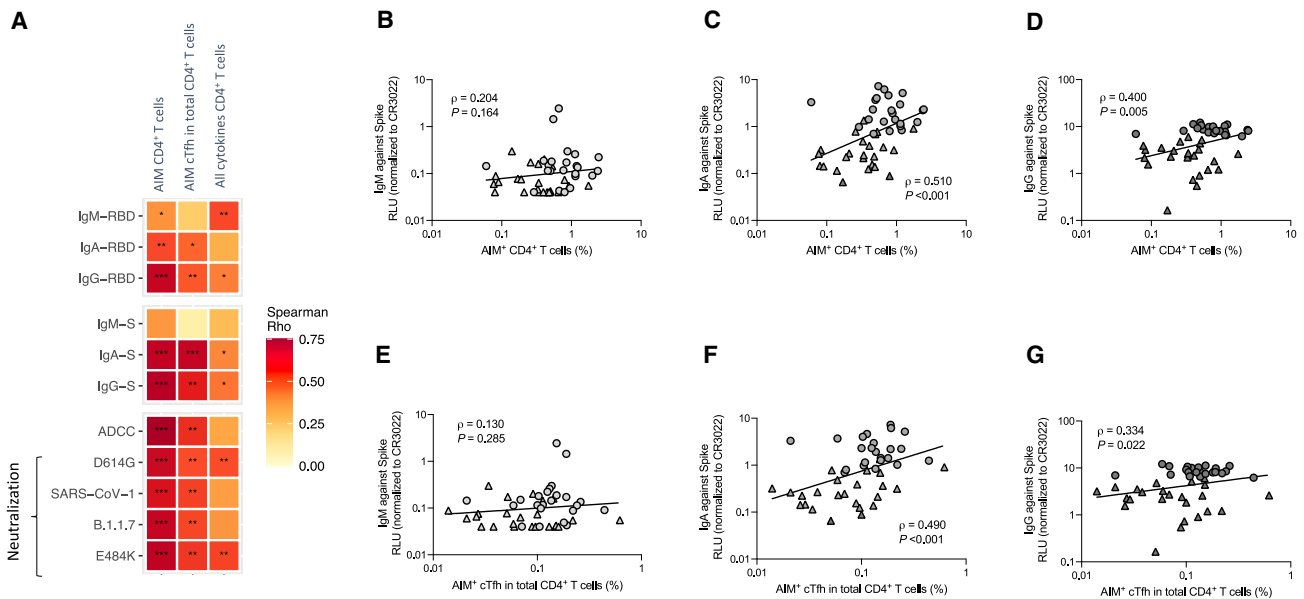


Figure 5. Total spike-specific CD4⁺ T cells and spike-specific cTfh responses at baseline correlate with humoral responses after vaccination (A) Heatmap showing associations between total S-specific CD4⁺ T cell or S-specific cTfh responses at baseline (V0) and Abs (against RBD and S), ADCC and neutralization functions after vaccination (V1). Color represents Rho value for each association calculated (Spearman correlation), and significant p values were indicated by * (for <0.05; ** for <0.01, and *** for <0.001). (B and E) Absence of significant correlations between IgM against S and AIM⁺ CD4⁺ T cells (B) and AIM⁺ cTfh responses (E). (C and F) Positive correlations between IgA against S and AIM⁺ CD4⁺ T cells (C) and AIM⁺ cTfh responses (F). (D and G) Positive correlation between IgG against S and AIM⁺ CD4⁺ T cells (D) and AIM⁺ cTfh responses (G). AIM⁺ cells were measured by flow cytometry and Abs were quantified by CBE. Each symbol identifies one donor (SARS-CoV-2 naive donors are represented by triangles and PI donors by circles).

T cell measurements and Ab responses were generally stronger than between ICS⁺ CD4⁺ T cell responses and serological measurements (Figure 5A). Notably, the Ig subsets measured after vaccination in the plasma of each participant showed significant positive correlations between pre-existing S-specific CD4⁺ T cell and cTfh responses on the one hand, and anti-S IgA and IgG post-vaccination on the other hand (Figure 5C, 5D, 5F, and 5G). In contrast, we observed no significant correlations between total S-specific CD4⁺ T cell responses and anti-S IgM levels (Figure 5B) and between S-specific cTfh responses and anti-S IgM levels (Figure 5E). At the functional level, we observed significant correlations between all the pre-vaccination AIM⁺ S-specific memory CD4⁺ T cells and cTfh with ADCC and neutralization capacity post-immunization (Figure 5A).

These results suggest that pre-existing CD4⁺ T cell responses are beneficial for the generation of specific and effective humoral responses against SARS-CoV-2 after a single dose of mRNA vaccine, independently of prior SARS-CoV-2 infection.

Evaluation of vaccine responses

Assessing the humoral responses revealed that the vaccine-induced responses in naive individuals show striking similarities with the induced responses upon natural infection. With a few exceptions such as the neutralizing Ab response, at least for the given time points, the induced responses are similar (Figures 1, 2, and 3). This translates into a similar network of pairwise correlations among all studied parameters when comparing discrete time points before vaccination in infected individuals

(D and E) Net frequencies of total S-specific responses measured by ICS for (D) CD4⁺ and (E) CD8⁺ T cells for each donor prior to and post vaccination. ICS⁺ populations include cells that expressed at least one cytokine and effector function (CD40L, CD107a, IFN- γ , IL-2, IL-10, and TNF- α for CD4⁺; CD107a, IFN- γ , IL-2, IL-10, and TNF- α for CD8⁺ T cells).

In (A–E), net frequency of the S-stimulated condition was calculated by subtracting the frequency detected in a DMSO control; bars correspond to median values, and symbols represent biologically independent samples from $n = 24$ SARS-CoV-2 naive individuals and $n = 24$ SARS-CoV-2 individuals with prior infection; lines connect data from the same donor.

(F and G) Analysis of the polyfunctionality of S-specific (F) CD4⁺ and (G) CD8⁺ T cells measured by ICS at the post-vaccination (V1) time point. Data were analyzed by combinatorial gates based on the coexpression of CD40L, CD107a, IFN- γ , IL-2, IL-10, and TNF- α for CD4⁺ and CD107a, IFN- γ , IL-2, IL-10, and TNF- α for CD8⁺ T cells. Box-and-whisker plots show median values (line), 25th to 75th percentiles (box outline), and minimum and maximum values (whiskers). In (F and G), net frequency responses greater than 2-fold over DMSO control (background) were considered; significant p values were indicated by * for <0.05, ** for <0.01, *** for <0.001, and **** for <0.0001.

P values were calculated by paired two-tailed Wilcoxon test for comparisons between the V0 and V1 time points in the same individual and Mann-Whitney test for comparisons between the two cohorts at either the V0 or the V1 time point (A–E). Comparisons between the polyfunctionality patterns were calculated using Mann-Whitney test (F–G).

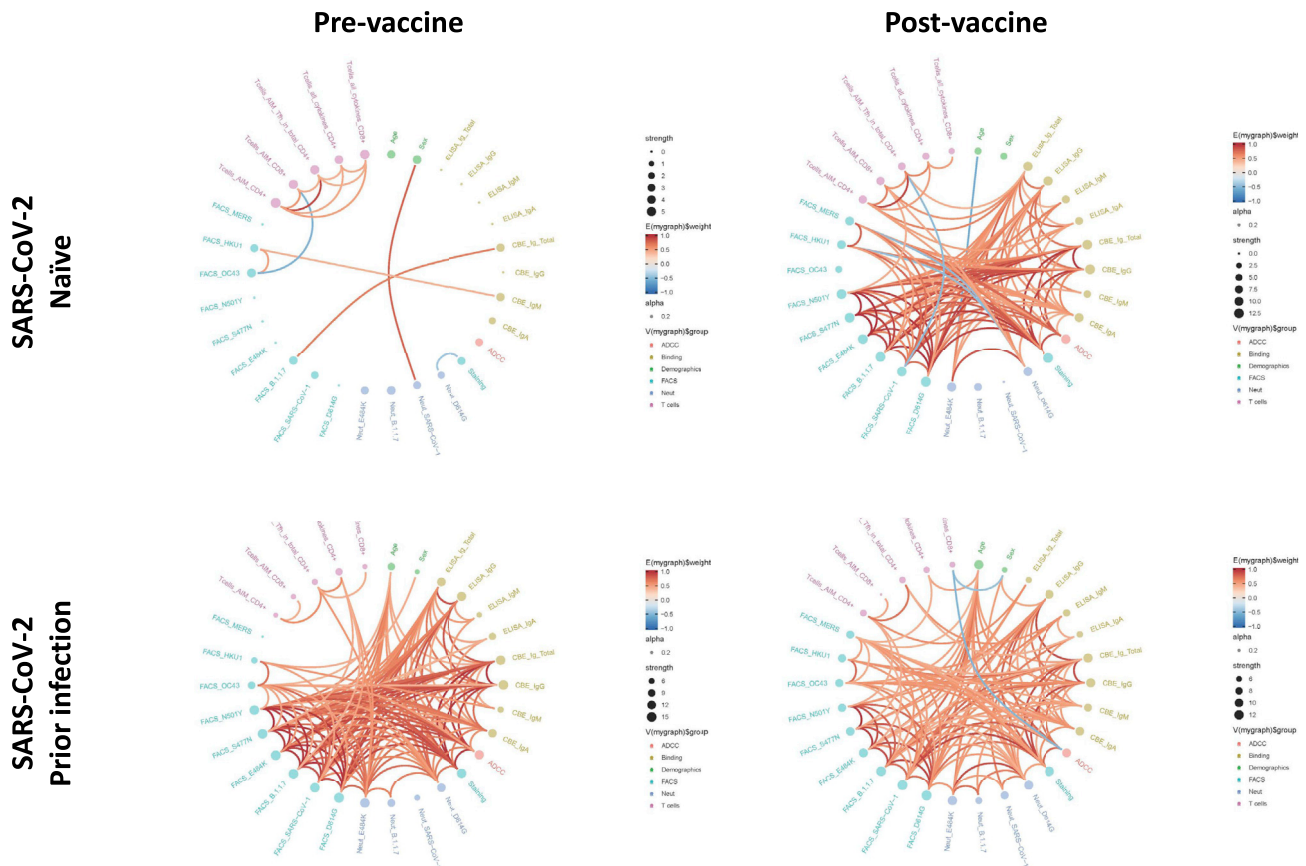


Figure 6. Mesh of correlations of humoral and cellular parameters at discrete time points before and after vaccination in SARS-CoV-2 naïve versus previously infected individuals

Edge bundling correlation plots where red and blue edges represent positive and negative correlations between connected parameters, respectively. Only significant correlations ($p < 0.05$, Spearman rank test) are displayed. Nodes are color coded based on the grouping of parameters according to the legend. Node size corresponds to the degree of relatedness of correlations. Edge bundling plots are shown for correlation analyses using four different datasets; i.e., SARS-CoV-2 naïve and PI individuals before and after vaccination, respectively.

and post-vaccination in naïve individuals (Figure 6). As expected, naïve individuals before vaccination harbor hardly any interrelations between humoral and cellular anti-SARS-CoV-2 responses, which is in line with their overall low and unspecific absolute levels. Notably, when studying the effects of vaccination in PI individuals, the pairwise correlations are not getting stronger among our studied parameters, but the network of significant associations is broadened involving more interconnected parameters. It indicates that a heterogeneous boost, in this case an S mRNA vaccination boost upon natural infection as prime, brings in new flavors of host responses while diluting others.

To investigate whether pre-existing humoral responses before vaccination predict the levels of induced/boosted responses upon vaccination, we performed a tandem correlation analysis focusing on pairs of correlations between time points before versus after vaccination (Figure S4). In naïve individuals, as expected, the low and SARS-CoV-2-unspecific responses before vaccination didn't predict responses induced by vaccination. In contrast, individuals with previous SARS-CoV-2 infection harbor a much broader set of parameters pre-vaccination that predict induced responses post-vaccination in the studied dataset.

Of interest, these correlations differ from the few observed in naïve individuals. In PI individuals, most prominent patterns include the predictive value of binding, ADCC, and neutralization responses pre-vaccination for IgA responses in CBE assays and neutralization against viruses with the E484K S escape mutation post-vaccination.

DISCUSSION

The mRNA vaccines have demonstrated a >90% efficacy starting 14 days after a single dose, but the immune correlate of protection after a single dose remains unknown (Baden et al., 2021; Polack et al., 2020; Skowronski et al., 2021). Here, we measured several serological and cellular SARS-CoV-2-specific responses in SARS-CoV-2 naïve or PI individuals. Surprisingly, despite the proven vaccine efficacy 3 weeks after vaccination (Baden et al., 2021; Polack et al., 2020; Skowronski et al., 2021), we observed weak neutralizing activity in plasma from SARS-CoV-2 naïve vaccinated individuals, in agreement with recent studies (Collier et al., 2021; Ellebedy et al., 2021; Goel et al., 2021; Planas et al., 2021; Sahin et al., 2020b). Neutralization is thought to play a

central role in SARS-CoV-2 vaccine efficacy (Jackson et al., 2020; Muruato et al., 2020; Polack et al., 2020); however, recent observations suggest that they might not be predictive, on their own, of protection (Emary et al., 2021; Luchsinger and Hillyer, 2021). Affinity maturation through GC selection can lead to more potent neutralizing Ab responses. While kinetics may differ according to the antigen used and route of administration, measurable neutralizing titers may take several weeks to develop in humans and NHPs after immunization (Cirelli et al., 2019), and even after neutralization titers begin to decrease, the somatic hypermutation (SHM) process can continue for months after acute SARS-CoV-2 infection (Gaebler et al., 2021). Our results suggest that while the neutralization potency of vaccine-elicited Abs is being developed, other Ab functions such as Fc-mediated effector functions could contribute to vaccine efficacy early on. Accordingly, 3 weeks after a single dose, we observed strong ADCC but weak neutralization activity (Figure 3). Vaccination induced strong levels of IgG in both groups, thus it would be interesting to study which subclasses of IgG were induced and if it correlates with the effector functions observed. Strikingly, vaccination of PI individuals induced a very significant increase of pre-existing humoral immunity including ADCC and neutralization. These results are consistent with several recent studies which have shown that a single vaccine dose in PI individuals led to similar humoral responses compared with two vaccine doses in naive individuals, and they suggest that the second dose may not be necessary for PI individuals (Ebinger et al., 2021; Krammer et al., 2021; Saadat et al., 2021). Neutralization potency was increased, enabling neutralization of several variants including the B.1.1.7 variant, S with the E484K mutation, and even the phylogenetically more distant SARS-CoV-1.

We also demonstrated that the patterns of vaccine-induced T cell responses have analogies with those observed for Ab immunity. A single dose of BNT162b2 mRNA vaccine is also capable of generating SARS-CoV-2-specific T cell immune responses in both groups of individuals with a dominant CD4⁺ T cell response, suggesting efficacy of the priming immunization in generating cellular immunity against SARS-CoV-2 S. However, we observed differences in the magnitude and quality of these responses between participants with and without prior infection. Individuals who had already encountered SARS-CoV-2 developed strong S-specific memory CD4⁺ and CD8⁺ T cells, consistent with secondary memory responses to a recall antigen. In contrast, naive individuals showed significantly weaker S-specific CD4⁺ T cell responses and low to undetectable S-specific CD8⁺ T cell responses by AIM and ICS. Even though pre-vaccination T cell responses to SARS-CoV-2 S glycoprotein were minimal in most naive participants, it is still possible that the vaccine amplifies pre-existing CD4⁺ cross-reactive T cell responses to endemic human coronaviruses. This suggests that a single dose of mRNA vaccine may be sufficient to elicit robust protective T cell responses in PI individuals; naive persons will likely benefit most from repeat immunization.

Our results support the parallel use of both AIM and ICS assays for SARS-CoV-2 vaccine immunomonitoring. While most clinical trials relied on the IFN- γ ELISPOT assay and/or ICS to measure T cell responses, our data suggest the notion that BNT162b2 and some other SARS-CoV-2 vaccines in advanced

clinical evaluation, including non-mRNA-vaccines, preferentially elicit Th1 responses and may have to be reconsidered (Corbett et al., 2020; van Doremalen et al., 2020; Ewer et al., 2021; Laczko et al., 2020; Zhang et al., 2020). Indeed, these assays are sensitive for detection of Th1 cytokines and cytotoxic responses, but largely miss other important components of virus-specific cellular immunity. Consistent with this, we found that AIM assays were highly sensitive to detect vaccine-induced CD4⁺ and CD8⁺ T cells, consistent with recent findings in natural SARS-CoV-2 infection and vaccination (Dan et al., 2021; Kalimuddin et al., 2021). Still, ICS assays were essential to reveal qualitative differences in cellular responses elicited after vaccination in PI versus naive participants, with more proinflammatory and antiviral CD4⁺ and CD8⁺ T cell functional profiles in almost all PI individuals, including IFN- γ , TNF- α , and for the CD8⁺ T cells, cytotoxic functions. Based on current knowledge, we suggest that a balanced humoral and Th1-directed cellular immune response may be important for protection from COVID-19 and the development of effective vaccine-induced immunization.

S-specific CD4⁺ T cell responses clearly dominated over CD8⁺ T cell responses, both for AIM and ICS measurements. Because of their role in antigen-specific B cell survival and maturation, we studied the correlation of CD4⁺ T cell responses with Ab immunity. We found strong positive correlations between S-specific AIM⁺ CD4⁺ T cell responses measured before vaccination and isotype-switched IgA and IgG Ab responses after vaccination, as well as ADCC and neutralization functions, contrasting with no significant correlations with the unswitched IgM responses. These patterns suggest that pre-existing memory T cell help is a major modulator of humoral SARS-CoV-2 vaccine responses. While the patterns of predictive associations were overall similar for total AIM⁺CD4⁺ T cells and AIM⁺ cTfh, the correlations were weaker with ICS measurements. Again, this suggests that the widely used ICS assays likely miss CD4⁺ T cell subsets that are important to sustain the development of vaccine Ab responses. Consistent with our observations on robust cTfh induction by BNT162b2 mRNA, it was shown that SARS-CoV-2 mRNA vaccine had a superior capacity, in comparison to rRBD-AddaVax, to elicit potent SARS-CoV-2-specific GC B cell responses after the administration of a single vaccine dose, suggesting that GC B cells and Tfh cells strongly correlated with the production of protective SARS-CoV-2-specific Ab responses (Lederer et al., 2020). Our results are also consistent with recent observations in convalescent COVID-19 donors, with reported correlations between antigen-specific CD4⁺ T cells (Grifoni et al., 2020) and cTfh cells (Mathew et al., 2020) and SARS-CoV-2-specific Abs. As the CD4 help-dependent development of high-affinity Ab responses is a desired outcome after vaccination, our results provide clear rationales for assessing CD4⁺ T cell responses as part of the evaluation of SARS-CoV-2 vaccine immunogenicity and durability of protection and for including function-agnostic techniques such as the AIM assays.

The availability of longitudinal sampling with six time points starting from a few weeks PSO up to 3 weeks post-vaccination enabled us to investigate the predictive capacity of distinct time points in infected/convalescent individuals for vaccine outcome in terms of humoral responses (Figure S5). At the earliest time point, a few weeks PSO, the predictive power of the studied parameters neutralization, ADCC, and ELISA binding

responses (IgA, IgG, IgM, and total Ig) were low; however, starting from time point 2, total Ig, IgG, and ADCC responses gain power to significantly predict stronger IgG responses post-vaccination. At the latest time point PSO, the predictive capacity of IgG and total Ig were partly diluted, but overall broadened, including predictions toward stronger IgA and IgM responses post-vaccination.

We note that vaccination of SARS-CoV-2 naive individuals with a mRNA vaccine bring their SARS-CoV-2-specific humoral and T cell responses to similar levels than the ones presented in individuals that were infected around nine months ago. Recent studies showed that natural infection confers up to 80% of protection from re-infection (Hall et al., 2021; Lumley et al., 2021); however, whether the same immune responses than those elicited by vaccination confer this protection remains unknown. Also, whether these humoral and T cell responses are unique to mRNA vaccine or could be extended to non-mRNA vaccines remains to be determined. These results give support to the consideration by various jurisdictions of a widened interval between the first and second dose in the context of vaccine shortage to protect a larger proportion of the population. The United Kingdom has decided to wait up to 12 weeks before administering the second dose of SARS-CoV-2 vaccines (Voysey et al., 2021), whereas Canada extended this interval up to 16 weeks (Public Health Agency of Canada, 2021). This is also advocated in the United States in the context of the surging B.1.1.7 variant (Osterholm et al., 2021).

While the duration of a protective immune response elicited by a single dose of mRNA vaccines is unknown, given that memory is a core function of the immune system, it is unlikely to decline within these intervals. Nevertheless, addressing this question will be very important as the larger the interval between doses is, the easier it will be to maximize the protection globally given the limited vaccine supply worldwide.

Limitations of study

Our results suggest that different antibody functions, beyond neutralization, could play a role in vaccine efficacy 3 weeks after a single dose of mRNA BNT162b2 vaccine in SARS-CoV-2 naive and PI individuals. A limitation of the study is that while we have shown that these humoral responses correlate with CD4 T cell responses, we don't know in which extent CD4 and CD8 T cell responses directly contribute to vaccine efficacy, besides their helper role for antibody immunity. Additional studies will be required to understand the role of T cell-mediated immunity in mRNA vaccine efficacy.

STAR★METHODS

Detailed methods are provided in the online version of this paper and include the following:

- **KEY RESOURCES TABLE**
- **RESOURCE AVAILABILITY**
 - Lead contact
 - Materials availability
 - Data and code availability
- **EXPERIMENTAL MODEL AND SUBJECT DETAILS**
 - Ethics statement

- Human subjects
- Plasma and antibodies
- Cell lines
- **METHOD DETAILS**
 - Plasmids
 - Protein expression and purification
 - Enzyme-linked immunosorbent assay (ELISA)
 - Cell-based ELISA
 - Cell surface staining and flow cytometry analysis
 - ADCC assay
 - Viral infectivity
 - Virus neutralization assay
 - Intracellular cytokine staining
 - Activation-induced marker assay
- **QUANTIFICATION AND STATISTICAL ANALYSIS**
 - Statistical analysis
 - Software scripts and visualization

SUPPLEMENTAL INFORMATION

Supplemental information can be found online at <https://doi.org/10.1016/j.chom.2021.06.001>.

ACKNOWLEDGMENTS

The authors are grateful to the donors who participated in this study. The authors thank the CRCHUM BSL3 and Flow Cytometry Platforms for technical assistance. We thank Annie Moisan, Gilles Turcotte, and Sclérodermie Québec for their generous support in the acquisition of the FACSymphony. We thank Dr. Stefan Pöhlmann (Georg-August University, Germany) for the plasmid coding for SARS-CoV-2 and SARS-CoV-1 S glycoproteins and Dr. M. Gordon Joyce (US MHRP) for the monoclonal antibody CR3022. The graphical abstract was prepared using images from [BioRender.com](https://www.biorender.com). This work was supported by le Ministère de l'Économie et de l'Innovation du Québec, Programme de Soutien aux Organismes de Recherche et d'Innovation to A.F. and by the Fondation du CHUM. This work was also supported by CIHR foundation grant 352417 to A.F., and by Exceptional Fund COVID-19 from the Canada Foundation for Innovation (CFI) 41027 to A.F. and D.E.K. Work on variants presented here was supported by the Sentinelle COVID Quebec network led by the LSPQ in collaboration with Fonds de Recherche du Québec Santé (FRQS) to A.F., and Genome Canada – Génome Québec to M.R. Support was also provided by NIH AI144462 CHAVD to D.E.K. (consortium PI: Dennis Burton). A.F. is the recipient of Canada Research Chair on Retroviral Entry no. RCHS0235 950-232424. V.M.-L. is supported by a FRQS Junior 1 salary award. D.E.K. is an FRQS Merit Research scholar. R.D. was supported by NIH grant R01 AI122953-05. S.P.A., J.P., and G.B.-B. are supported by CIHR fellowships. R.G. is supported by a MITACS Accélération postdoctoral fellowship. The funders had no role in study design, data collection and analysis, decision to publish, or preparation of the manuscript.

AUTHOR CONTRIBUTIONS

A.T., M.N., D.E.K., and A.F. conceived the study. A.T., M.N., R.G., G.B.B., J.P., S.P.A., J.N., J.R., D.E.K., and A.F. designed experimental approaches. A.T., M.N., M.B., S.Y.G., R.G., G.B.B., N.B., D.V., J.P., S.P.A., C.B., J.R., D.E.K., and A.F. performed, analyzed, and interpreted the experiments. A.T., M.N., R.D., and O.T. performed statistical analysis. S.Y.G., A.L., J.P., H.M., G.G.L., G.G., L.S., A.T.M., P.U., M.L., W.M., J.R., and A.F. contributed unique reagents. L.G., C.M., P.A., V.M.-L., and C.T. collected clinical samples. C.L., G.D.S., S.M., and M.R. provided scientific input related to VOC. A.T., M.N., D.E.K., and A.F. wrote the manuscript with inputs from others. Every author has read, edited, and approved the final manuscript.

DECLARATION OF INTERESTS

The authors declare no competing interests.

Received: March 22, 2021

Revised: May 6, 2021

Accepted: June 1, 2021

Published: June 4, 2021

REFERENCES

- Anand, S.P., Prévost, J., Richard, J., Perreault, J., Tremblay, T., Drouin, M., Fournier, M.-J., Lewin, A., Bazin, R., and Finzi, A. (2021a). High-throughput detection of antibodies targeting the SARS-CoV-2 Spike in longitudinal convalescent plasma samples. *Transfusion* **61**, 1377–1382.
- Anand, S.P., Prévost, J., Nayrac, M., Beaudoin-Bussièrès, G., Benlarbi, M., Gasser, R., Brassard, N., Laumaea, A., Gong, S.Y., Bourassa, C., et al. (2021b). Longitudinal analysis of humoral immunity against SARS-CoV-2 Spike in convalescent individuals up to 8 months post-symptom onset. *BioRxiv*. <https://doi.org/10.1101/2021.01.25.428097>.
- Baden, L.R., El Sahly, H.M., Essink, B., Kotloff, K., Frey, S., Novak, R., Diemert, D., Spector, S.A., Roupshael, N., Creech, C.B., et al.; COVE Study Group (2021). Efficacy and Safety of the mRNA-1273 SARS-CoV-2 Vaccine. *N. Engl. J. Med.* **384**, 403–416.
- Beaudoin-Bussièrès, G., Laumaea, A., Anand, S.P., Prévost, J., Gasser, R., Goyette, G., Medjahed, H., Perreault, J., Tremblay, T., Lewin, A., et al. (2020). Decline of Humoral Responses against SARS-CoV-2 Spike in Convalescent Individuals. *MBio* **11**. <https://doi.org/10.1128/mBio.02590-20>.
- Breton, G., Mendoza, P., Hägglöf, T., Oliveira, T.Y., Schaefer-Babajew, D., Gaebler, C., Turroja, M., Hurley, A., Caskey, M., and Nussenzweig, M.C. (2021). Persistent cellular immunity to SARS-CoV-2 infection. *J. Exp. Med.* **218**. <https://doi.org/10.1101/2020.12.08.416636>.
- Chan, C.E.Z., Seah, S.G.K., Chye, D.H., Massey, S., Torres, M., Lim, A.P.C., Wong, S.K.K., Neo, J.J.Y., Wong, P.S., Lim, J.H., et al. (2020a). The Fc-mediated effector functions of a potent SARS-CoV-2 neutralizing antibody, SC31, isolated from an early convalescent COVID-19 patient, are essential for the optimal therapeutic efficacy of the antibody. *bioRxiv*. <https://doi.org/10.1101/2020.10.26.355107>.
- Chan, K.K., Tan, T.J.C., Narayanan, K.K., and Procko, E. (2020b). An engineered decoy receptor for SARS-CoV-2 broadly binds protein S sequence variants. *BioRxiv*. <https://doi.org/10.1126/sciadv.abf1738>.
- Cirelli, K.M., Carnathan, D.G., Nogal, B., Martin, J.T., Rodriguez, O.L., Upadhyay, A.A., Enemu, C.A., Geburu, E.H., Choe, Y., Viviano, F., et al. (2019). Slow Delivery Immunization Enhances HIV Neutralizing Antibody and Germinal Center Responses via Modulation of Immunodominance. *Cell* **177**, 1153–1171.e28.
- Collier, D.A., De Marco, A., Ferreira, I.A.T.M., Meng, B., Datt, R.P., Walls, A.C., Kemp, S.A., Bassi, J., Pinto, D., Silacci-Fregni, C., et al.; CITIID-NIHR BioResource COVID-19 Collaboration; COVID-19 Genomics UK (COG-UK) Consortium (2021). Sensitivity of SARS-CoV-2 B.1.1.7 to mRNA vaccine-elicited antibodies. *Nature* **593**, 136–141.
- Corbett, K.S., Edwards, D.K., Leist, S.R., Abiona, O.M., Boyoglu-Barnum, S., Gillespie, R.A., Himansu, S., Schäfer, A., Ziwawo, C.T., DiPiazza, A.T., et al. (2020). SARS-CoV-2 mRNA vaccine design enabled by prototype pathogen preparedness. *Nature* **586**, 567–571.
- Corum, J., and Zimmer, C. (2021). Inside the B.1.1.7 Coronavirus Variant (The New York Times), January 18, 2021. <https://www.nytimes.com/interactive/2021/health/coronavirus-mutations-B117-variant.html>.
- Crotty, S. (2014). T follicular helper cell differentiation, function, and roles in disease. *Immunity* **41**, 529–542.
- Dan, J.M., Lindestam Arleham, C.S., Weiskopf, D., da Silva Antunes, R., Havenar-Daughton, C., Reiss, S.M., Brigger, M., Bothwell, M., Sette, A., and Crotty, S. (2016). A Cytokine-Independent Approach To Identify Antigen-Specific Human Germinal Center T Follicular Helper Cells and Rare Antigen-Specific CD4+ T Cells in Blood. *J. Immunol.* **197**, 983–993.
- Dan, J.M., Mateus, J., Kato, Y., Hastie, K.M., Yu, E.D., Faliti, C.E., Grifoni, A., Ramirez, S.I., Haupt, S., Frazier, A., et al. (2021). Immunological memory to SARS-CoV-2 assessed for up to 8 months after infection. *Science* **371**, eabf4063.
- Davies, N.G., Barnard, R.C., Jarvis, C.I., Kucharski, A.J., Munday, J., Pearson, C.A.B., Russell, T.W., Tully, D.C., Abbott, S., Gimma, A., et al. (2020). Estimated transmissibility and severity of novel SARS-CoV-2 Variant of Concern 202012/01 in England. *MedRxiv*. <https://doi.org/10.1101/2020.12.24.20248822>.
- Dong, E., Du, H., and Gardner, L. (2020). An interactive web-based dashboard to track COVID-19 in real time. *Lancet Infect. Dis.* **20**, 533–534.
- Ebinger, J.E., Fert-Bober, J., Printsev, I., Wu, M., Sun, N., Prostko, J.C., Frias, E.C., Stewart, J.L., Van Eyk, J.E., Braun, J.G., et al. (2021). Antibody responses to the BNT162b2 mRNA vaccine in individuals previously infected with SARS-CoV-2. *Nat. Med.* <https://doi.org/10.1038/s41591-021-01325-6>.
- Ellebedy, A., Turner, J., O'Halloran, J., Kalaidina, E., Kim, W., Schmitz, A., Lei, T., Thapa, M., Chen, R., Case, J., et al. (2021). SARS-CoV-2 mRNA vaccines induce a robust germinal center reaction in humans. *Nature Portfolio*. <https://doi.org/10.21203/rs.3.rs-310773/v1>.
- Emary, K.R.W., Golubchik, T., Aley, P.K., Ariani, C.V., Angus, B.J., Bibi, S., Blane, B., Bonsall, D., Cicconi, P., Charlton, S., et al. (2021). Efficacy of ChAdOx1 nCoV-19 (AZD1222) Vaccine Against SARS-CoV-2 VOC 202012/01 (B.1.1.7) (SSRN Electron. J.).
- Ewer, K.J., Barrett, J.R., Belij-Rammerstorfer, S., Sharpe, H., Makinson, R., Morter, R., Flaxman, A., Wright, D., Bellamy, D., Bittaye, M., et al.; Oxford COVID Vaccine Trial Group (2021). T cell and antibody responses induced by a single dose of ChAdOx1 nCoV-19 (AZD1222) vaccine in a phase 1/2 clinical trial. *Nat. Med.* **27**, 270–278.
- Flores-Alanis, A., Cruz-Rangel, A., Rodríguez-Gómez, F., González, J., Torres-Guerrero, C.A., Delgado, G., Cravioto, A., and Morales-Espinosa, R. (2021). Molecular Epidemiology Surveillance of SARS-CoV-2: Mutations and Genetic Diversity One Year after Emerging. *Pathogens* **10**. <https://doi.org/10.3390/pathogens10020184>.
- Gaebler, C., Wang, Z., Lorenzi, J.C.C., Muecksch, F., Finkin, S., Tokuyama, M., Cho, A., Jankovic, M., Schaefer-Babajew, D., Oliveira, T.Y., et al. (2021). Evolution of antibody immunity to SARS-CoV-2. *Nature* **591**, 639–644.
- Gasser, R., Cloutier, M., Prévost, J., Fink, C., Ducas, E., Ding, S., Dussault, N., Landry, P., Tremblay, T., Laforce-Lavoie, A., et al. (2021). Major role of IgM in the neutralizing activity of convalescent plasma against SARS-CoV-2. *Cell Rep.* **34**, 108790.
- Goel, R.R., Apostolidis, S.A., Painter, M.M., Mathew, D., Pattekar, A., Kuthuru, O., Gouma, S., Hicks, P., Meng, W., Rosenfeld, A.M., et al. (2021). Distinct antibody and memory B cell responses in SARS-CoV-2 naïve and recovered individuals following mRNA vaccination. *Sci. Immunol.* **6**, eabi6950.
- Grifoni, A., Weiskopf, D., Ramirez, S.I., Mateus, J., Dan, J.M., Moderbacher, C.R., Rawlings, S.A., Sutherland, A., Premkumar, L., Jadi, R.S., et al. (2020). Targets of T Cell Responses to SARS-CoV-2 Coronavirus in Humans with COVID-19 Disease and Unexposed Individuals. *Cell* **181**, 1489–1501.e15.
- Gröhs Ferrareze, P.A., Franceschi, V.B., de Menezes Mayer, A., Caldana, G.D., Zimmer, R.A., and Thompson, C.E. (2021). E484K as an innovative phylogenetic event for viral evolution: Genomic analysis of the E484K spike mutation in SARS-CoV-2 lineages from Brazil. *BioRxiv*. <https://doi.org/10.1101/2021.01.27.426895>.
- Hall, V.J., Foulkes, S., Charlett, A., Atti, A., Monk, E.J., Simmons, R., Wellington, E., Cole, M., Saei, A., Oguti, B., et al. (2021). Do Antibody Positive Healthcare Workers Have Lower SARS-CoV-2 Infection Rates than Antibody Negative Healthcare Workers? Large Multi-Centre Prospective Cohort Study (The SIREN Study), England: June to November 2020 (Rochester, NY: Social Science Research Network).
- Heit, A., Schmitz, F., Gerdts, S., Flach, B., Moore, M.S., Perkins, J.A., Robins, H.S., Aderem, A., Spearman, P., Tomaras, G.D., et al. (2017). Vaccination establishes clonal relatives of germinal center T cells in the blood of humans. *J. Exp. Med.* **214**, 2139–2152.
- Hodcroft, E.B., Zuber, M., Nadeau, S., Crawford, K.H.D., Bloom, J.D., Veessler, D., Vaughan, T.G., Comas, I., Candelas, F.G., Consortium, S.-S., et al. (2020).

Emergence and spread of a SARS-CoV-2 variant through Europe in the summer of 2020. *MedRxiv*. <https://doi.org/10.1101/2020.10.25.20219063>.

Hoffmann, M., Müller, M.A., Drexler, J.F., Glende, J., Erdt, M., Gützkow, T., Losemann, C., Binger, T., Deng, H., Schwegmann-Weßels, C., et al. (2013). Differential sensitivity of bat cells to infection by enveloped RNA viruses: coronaviruses, paramyxoviruses, filoviruses, and influenza viruses. *PLoS One* **8**, e72942.

Hoffmann, M., Kleine-Weber, H., Schroeder, S., Krüger, N., Herrler, T., Erichsen, S., Schiergens, T.S., Herrler, G., Wu, N.-H., Nitsche, A., et al. (2020). SARS-CoV-2 Cell Entry Depends on ACE2 and TMPRSS2 and Is Blocked by a Clinically Proven Protease Inhibitor. *Cell* **181**, 271–280.e8.

Isabel, S., Graña-Miraglia, L., Gutierrez, J.M., Bundalovic-Torma, C., Groves, H.E., Isabel, M.R., Eshaghi, A., Patel, S.N., Gubbay, J.B., Poutanen, T., et al. (2020). Evolutionary and structural analyses of SARS-CoV-2 D614G spike protein mutation now documented worldwide. *Sci. Rep.* **10**, 14031.

Jackson, L.A., Anderson, E.J., Roupheal, N.G., Roberts, P.C., Makhene, M., Coler, R.N., McCullough, M.P., Chappell, J.D., Denison, M.R., Stevens, L.J., et al.; mRNA-1273 Study Group (2020). An mRNA Vaccine against SARS-CoV-2 - Preliminary Report. *N. Engl. J. Med.* **383**, 1920–1931.

Jolly, B., Rophina, M., Shamnath, A., Imran, M., Bhojar, R.C., Divakar, M.K., Rani, P.R., Ranjan, G., Sehgal, P., Chandrasekhar, P., et al. (2021). Genetic epidemiology of variants associated with immune escape from global SARS-CoV-2 genomes. *BioRxiv*. <https://doi.org/10.1101/2020.12.24.424332>.

Ju, B., Zhang, Q., Ge, J., Wang, R., Sun, J., Ge, X., Yu, J., Shan, S., Zhou, B., Song, S., et al. (2020). Human neutralizing antibodies elicited by SARS-CoV-2 infection. *Nature* **584**, 115–119.

Kalimuddin, S., Tham, C.Y.L., Qui, M., de Alwis, R., Sim, J.X.Y., Lim, J.M.E., Tan, H.-C., Syenina, A., Zhang, S.L., Le Bert, N., et al. (2021). Early T cell and binding antibody responses are associated with COVID-19 RNA vaccine efficacy onset. *Med*. <https://doi.org/10.1016/j.medj.2021.04.003>.

Krammer, F. (2020). SARS-CoV-2 vaccines in development. *Nature* **586**, 516–527.

Krammer, F., Srivastava, K., Alshammary, H., Amoako, A.A., Awawda, M.H., Beach, K.F., Bermúdez-González, M.C., Bielak, D.A., Carreño, J.M., Chernet, R.L., et al. (2021). Antibody Responses in Seropositive Persons after a Single Dose of SARS-CoV-2 mRNA Vaccine. *N. Engl. J. Med.* **384**, 1372–1374.

Ku, Z., Xie, X., Davidson, E., Ye, X., Su, H., Menachery, V.D., Li, Y., Yuan, Z., Zhang, X., Muruato, A.E., et al. (2021). Molecular determinants and mechanism for antibody cocktail preventing SARS-CoV-2 escape. *Nat. Commun.* **12**, 469.

Laczkó, D., Hogan, M.J., Toulmin, S.A., Hicks, P., Lederer, K., Gaudette, B.T., Castaño, D., Amanat, F., Muramatsu, H., Oguin, T.H., 3rd, et al. (2020). A Single Immunization with Nucleoside-Modified mRNA Vaccines Elicits Strong Cellular and Humoral Immune Responses against SARS-CoV-2 in Mice. *Immunity* **53**, 724–732.e7.

Lederer, K., Castaño, D., Gómez Atria, D., Oguin, T.H., 3rd, Wang, S., Manzoni, T.B., Muramatsu, H., Hogan, M.J., Amanat, F., Cherubin, P., et al. (2020). SARS-CoV-2 mRNA Vaccines Foster Potent Antigen-Specific Germinal Center Responses Associated with Neutralizing Antibody Generation. *Immunity* **53**, 1281–1295.e5.

Luchsinger, L.L., and Hillyer, C.D. (2021). Vaccine efficacy probable against COVID-19 variants. *Science* **371**, 1116.

Lumley, S.F., O'Donnell, D., Stoesser, N.E., Matthews, P.C., Howarth, A., Hatch, S.B., Marsden, B.D., Cox, S., James, T., Warren, F., et al.; Oxford University Hospitals Staff Testing Group (2021). Antibody Status and Incidence of SARS-CoV-2 Infection in Health Care Workers. *N. Engl. J. Med.* **384**, 533–540.

Mathew, D., Giles, J.R., Baxter, A.E., Oldridge, D.A., Greenplate, A.R., Wu, J.E., Alanio, C., Kuri-Cervantes, L., Pampena, M.B., D'Andrea, K., et al.; UPenn COVID Processing Unit (2020). Deep immune profiling of COVID-19 patients reveals distinct immunotypes with therapeutic implications. *Science* **369**, eabc8511.

Mauri, M., Elli, T., Caviglia, G., Uboldi, G., and Azzi, M. (2017). RAWGraphs: A Visualisation Platform to Create Open Outputs. In *Proceedings of the 12th*

Biannual Conference on Italian SIGCHI Chapter (USA: Association for Computing Machinery), pp. 1–5.

Mejdani, M., Haddadi, K., Pham, C., and Mahadevan, R. (2021). SARS-CoV-2 receptor binding mutations and antibody mediated immunity. *BioRxiv*. <https://doi.org/10.1101/2021.01.25.427846>.

Moore, J.P., and Klasse, P.J. (2020). COVID-19 Vaccines: “Warp Speed” Needs Mind Melds, Not Warped Minds. *J. Virol.* **94**, e01083–20.

Morita, R., Schmitt, N., Bentebibel, S.-E., Ranganathan, R., Bourdery, L., Zurawski, G., Foucat, E., Dullaers, M., Oh, S., Sabzghabaei, N., et al. (2011). Human blood CXCR5(+)CD4(+) T cells are counterparts of T follicular cells and contain specific subsets that differentially support antibody secretion. *Immunity* **34**, 108–121.

Muñoz-Fontela, C., Dowling, W.E., Funnell, S.G.P., Gsell, P.-S., Riveros-Balta, A.X., Albrecht, R.A., Andersen, H., Baric, R.S., Carroll, M.W., Cavaleri, M., et al. (2020). Animal models for COVID-19. *Nature* **586**, 509–515.

Muruato, A.E., Fontes-Garfias, C.R., Ren, P., Garcia-Blanco, M.A., Menachery, V.D., Xie, X., and Shi, P.-Y. (2020). A high-throughput neutralizing antibody assay for COVID-19 diagnosis and vaccine evaluation. *Nat. Commun.* **11**, 4059.

Nelson, G., Buzko, O., Spilman, P., Niazi, K., Rabizadeh, S., and Soon-Shiong, P. (2021). Molecular dynamic simulation reveals E484K mutation enhances spike RBD-ACE2 affinity and the combination of E484K, K417N and N501Y mutations (501Y.V2 variant) induces conformational change greater than N501Y mutant alone, potentially resulting in an escape mutant. *BioRxiv*. <https://doi.org/10.1101/2021.01.13.426558>.

Niessi, J., Baxter, A.E., Mendoza, P., Jankovic, M., Cohen, Y.Z., Butler, A.L., Lu, C.-L., Dubé, M., Shimeliovich, I., Gruell, H., et al. (2020a). Combination anti-HIV-1 antibody therapy is associated with increased virus-specific T cell immunity. *Nat. Med.* **26**, 222–227.

Niessi, J., Baxter, A.E., Morou, A., Brunet-Ratnasingham, E., Sannier, G., Gendron-Lepage, G., Richard, J., Delgado, G.-G., Brassard, N., Turcotte, I., et al. (2020b). Persistent expansion and Th1-like skewing of HIV-specific circulating T follicular helper cells during antiretroviral therapy. *EBioMedicine* **54**, 102727.

Osterholm, M., Ulrich, A., Anderson, C., Topol, E., Gellin, B., Berkelman, R., Lipsitch, M., and Moore, K. Report 7: Reassessing COVID-19 Vaccine Deployment in Anticipation of a US B.1.1.7 Surge: Stay the Course or Pivot?. <https://www.cidrap.umn.edu/sites/default/files/public/downloads/cidrap-covid19-viewpoint-report7.pdf>.

Park, J.-E., Li, K., Bartan, A., Fehr, A.R., Perlman, S., McCray, P.B., Jr., and Gallagher, T. (2016). Proteolytic processing of Middle East respiratory syndrome coronavirus spikes expands virus tropism. *Proc. Natl. Acad. Sci. USA* **113**, 12262–12267.

Planas, D., Bruel, T., Grzelak, L., Guivel-Benhassine, F., Staropoli, I., Porrot, F., Planchais, C., Buchrieser, J., Rajah, M.M., Bishop, E., et al. (2021). Sensitivity of infectious SARS-CoV-2 B.1.1.7 and B.1.351 variants to neutralizing antibodies. *BioRxiv*. <https://doi.org/10.1101/2021.02.12.430472>.

Polack, F.P., Thomas, S.J., Kitchin, N., Absalon, J., Gurtman, A., Lockhart, S., Perez, J.L., Pérez Marc, G., Moreira, E.D., Zerbini, C., et al.; C4591001 Clinical Trial Group (2020). Safety and Efficacy of the BNT162b2 mRNA Covid-19 Vaccine. *N. Engl. J. Med.* **383**, 2603–2615.

Prévost, J., and Finzi, A. (2021). The great escape? SARS-CoV-2 variants evading neutralizing responses. *Cell Host Microbe* **29**, 322–324.

Prévost, J., Gasser, R., Beaudoin-Bussièrès, G., Richard, J., Duerr, R., Laumaea, A., Anand, S.P., Goyette, G., Benlarbi, M., Ding, S., et al. (2020). Cross-Sectional Evaluation of Humoral Responses against SARS-CoV-2 Spike. *Cell Rep. Med.* **1**, 100126.

Public Health Agency of Canada (2021). NACI rapid response: Extended dose intervals for COVID-19 vaccines to optimize early vaccine rollout and population protection in Canada. <https://www.canada.ca/en/public-health/services/immunization/national-advisory-committee-on-immunization-naci/rapid-response-extended-dose-intervals-covid-19-vaccines-early-rollout-population-protection.html>.

- Pulendran, B., and Ahmed, R. (2011). Immunological mechanisms of vaccination. *Nat. Immunol.* **12**, 509–517.
- R: A language and environment for statistical computing. <https://www.gbif.org/fr/tool/81287/r-a-language-and-environment-for-statistical-computing>.
- RStudio: Open source & professional software for data science teams. <https://rstudio.com/>.
- Rambaut, A., Loman, N., Pybus, O., Barclay, W., Barrett, J., Carabelli, A., Connor, T., Peacock, T., Robertson, D.L., and Volz, E. (2020). Preliminary genomic characterisation of an emergent SARS-CoV-2 lineage in the UK defined by a novel set of spike mutations. <https://virological.org/t/preliminary-genomic-characterisation-of-an-emergent-sars-cov-2-lineage-in-the-uk-defined-by-a-novel-set-of-spike-mutations/563>.
- Reiss, S., Baxter, A.E., Cirelli, K.M., Dan, J.M., Morou, A., Daigneault, A., Brassard, N., Silvestri, G., Routy, J.-P., Havenar-Daughton, C., et al. (2017). Comparative analysis of activation induced marker (AIM) assays for sensitive identification of antigen-specific CD4 T cells. *PLoS One* **12**, e0186998.
- Rydzynski Moderbacher, C., Ramirez, S.I., Dan, J.M., Grifoni, A., Hastie, K.M., Weiskopf, D., Belanger, S., Abbott, R.K., Kim, C., Choi, J., et al. (2020). Antigen-Specific Adaptive Immunity to SARS-CoV-2 in Acute COVID-19 and Associations with Age and Disease Severity. *Cell* **183**, 996–1012.e19.
- Saadat, S., Rikhtegaran Tehrani, Z., Logue, J., Newman, M., Frieman, M.B., Harris, A.D., and Sajadi, M.M. (2021). Binding and Neutralization Antibody Titers After a Single Vaccine Dose in Health Care Workers Previously Infected With SARS-CoV-2. *JAMA* **325**, 1467–1469.
- Sabino, E.C., Buss, L.F., Carvalho, M.P.S., Prete, C.A., Jr., Crispim, M.A.E., Fraiji, N.A., Pereira, R.H.M., Parag, K.V., da Silva Peixoto, P., Kraemer, M.U.G., et al. (2021). Resurgence of COVID-19 in Manaus, Brazil, despite high seroprevalence. *Lancet* **397**, 452–455.
- Sahin, U., Muik, A., Derhovanessian, E., Vogler, I., Kranz, L.M., Vormehr, M., Baum, A., Pascal, K., Quandt, J., Maurus, D., et al. (2020a). COVID-19 vaccine BNT162b1 elicits human antibody and T_H1 T cell responses. *Nature* **586**, 594–599.
- Sahin, U., Muik, A., Vogler, I., Derhovanessian, E., Kranz, L.M., Vormehr, M., Quandt, J., Bidmon, N., Ulges, A., Baum, A., et al. (2020b). BNT162b2 induces SARS-CoV-2-neutralising antibodies and T cells in humans. *medRxiv*. <https://doi.org/10.1101/2020.12.09.20245175>.
- Sallusto, F., Lanzavecchia, A., Araki, K., and Ahmed, R. (2010). From vaccines to memory and back. *Immunity* **33**, 451–463.
- Schäfer, A., Muecksch, F., Lorenzi, J.C.C., Leist, S.R., Cipolla, M., Bournazos, S., Schmidt, F., Maison, R.M., Gazumyan, A., Martinez, D.R., et al. (2021). Antibody potency, effector function, and combinations in protection and therapy for SARS-CoV-2 infection in vivo. *J. Exp. Med.* **218**, e20201993.
- Sette, A., and Crotty, S. (2021). Adaptive immunity to SARS-CoV-2 and COVID-19. *Cell* **184**, 861–880.
- Skowronski, D., and De Serres, G. (2021). Safety and Efficacy of the BNT162b2 mRNA Covid-19 Vaccine. *N. Engl. J. Med.* **384**, 1576–1578.
- Skowronski, D., El Adam, S., Ouakki, M., Setayeshgar, S., Boulianne, N., Zou, M., Kiely, M., Fortin, E., De Wals, P., and De Serres, G. (2021). Données préliminaires sur l'efficacité vaccinale et avis complémentaire sur la stratégie de vaccination contre la COVID-19 au Québec en contexte de pénurie. https://inspq.qc.ca/sites/default/files/publications/3111_vaccination_covid19_2e_dose_contexte_penurie.pdf.
- Stamatatos, L., Czartoski, J., Wan, Y.-H., Homad, L.J., Rubin, V., Glantz, H., Neradilek, M., Seydoux, E., Jennewein, M.F., MacCamy, A.J., et al. (2021). Antibodies elicited by SARS-CoV-2 infection and boosted by vaccination neutralize an emerging variant and SARS-CoV-1. *medRxiv*. <https://doi.org/10.1101/2021.02.05.21251182>.
- Tada, T., Dcosta, B.M., Samanovic-Golden, M., Herati, R.S., Cornelius, A., Mulligan, M.J., and Landau, N.R. (2021). Neutralization of viruses with European, South African, and United States SARS-CoV-2 variant spike proteins by convalescent sera and BNT162b2 mRNA vaccine-elicited antibodies. *bioRxiv*. <https://doi.org/10.1101/2021.02.05.430003>.
- Tegally, H., Wilkinson, E., Giovanetti, M., Iranzadeh, A., Fonseca, V., Giandhari, J., Doolabh, D., Pillay, S., San, E.J., Msomi, N., et al. (2020). Emergence and rapid spread of a new severe acute respiratory syndrome-related coronavirus 2 (SARS-CoV-2) lineage with multiple spike mutations in South Africa. *medRxiv*. <https://doi.org/10.1101/2020.12.21.20248640>.
- van Doremalen, N., Lambe, T., Spencer, A., Belij-Rammerstorfer, S., Purushotham, J.N., Port, J.R., Avanzato, V.A., Bushmaker, T., Flaxman, A., Ulaszewska, M., et al. (2020). ChAdOx1 nCoV-19 vaccine prevents SARS-CoV-2 pneumonia in rhesus macaques. *Nature* **586**, 578–582.
- Vella, L.A., Buggert, M., Manne, S., Herati, R.S., Sayin, I., Kuri-Cervantes, L., Bukh Brody, I., O'Boyle, K.C., Kaprielian, H., Giles, J.R., et al. (2019). T follicular helper cells in human efferent lymph retain lymphoid characteristics. *J. Clin. Invest.* **129**, 3185–3200.
- Volz, E., Mishra, S., Chand, M., Barrett, J.C., Johnson, R., Geidelberg, L., Hinsley, W.R., Laydon, D.J., Dabrera, G., O'Toole, Á., et al. (2021). Transmission of SARS-CoV-2 Lineage B.1.1.7 in England: Insights from linking epidemiological and genetic data. *medRxiv*. <https://doi.org/10.1101/2020.12.30.20249034>.
- Voysey, M., Costa Clemens, S.A., Madhi, S.A., Weckx, L.Y., Folegatti, P.M., Aley, P.K., Angus, B., Baillie, V.L., Barnabas, S.L., Bhorat, Q.E., et al.; Oxford COVID Vaccine Trial Group (2021). Single-dose administration and the influence of the timing of the booster dose on immunogenicity and efficacy of ChAdOx1 nCoV-19 (AZD1222) vaccine: a pooled analysis of four randomised trials. *Lancet* **397**, 881–891.
- Walls, A.C., Park, Y.-J., Tortorici, M.A., Wall, A., McGuire, A.T., and Veesler, D. (2020). Structure, Function, and Antigenicity of the SARS-CoV-2 Spike Glycoprotein. *Cell* **181**, 281–292.e6.
- Wang, Z., Schmidt, F., Weisblum, Y., Muecksch, F., Barnes, C.O., Finkin, S., Schaefer-Babajew, D., Cipolla, M., Gaebler, C., Lieberman, J.A., et al. (2021). mRNA vaccine-elicited antibodies to SARS-CoV-2 and circulating variants. *Nature* **592**, 616–622.
- West, A.P., Barnes, C.O., Yang, Z., and Bjorkman, P.J. (2021). SARS-CoV-2 lineage B.1.526 emerging in the New York region detected by software utility created to query the spike mutational landscape. *bioRxiv*. <https://doi.org/10.1101/2021.02.14.431043>.
- World Health Organization. WHO Coronavirus (COVID-19) Dashboard. <https://covid19.who.int>.
- Wrapp, D., Wang, N., Corbett, K.S., Goldsmith, J.A., Hsieh, C.-L., Abiona, O., Graham, B.S., and McLellan, J.S. (2020). Cryo-EM structure of the 2019-nCoV spike in the prefusion conformation. *Science* **367**, 1260–1263.
- Wu, Y., Wang, F., Shen, C., Peng, W., Li, D., Zhao, C., Li, Z., Li, S., Bi, Y., Yang, Y., et al. (2020). A noncompeting pair of human neutralizing antibodies block COVID-19 virus binding to its receptor ACE2. *Science* **368**, 1274–1278.
- Wu, A., Wang, L., Zhou, H.-Y., Ji, C.-Y., Xia, S.Z., Cao, Y., Meng, J., Ding, X., Gold, S., Jiang, T., and Cheng, G. (2021). One year of SARS-CoV-2 evolution. *Cell Host Microbe* **29**, 503–507.
- Zhang, N.-N., Li, X.-F., Deng, Y.-Q., Zhao, H., Huang, Y.-J., Yang, G., Huang, W.-J., Gao, P., Zhou, C., Zhang, R.-R., et al. (2020). A Thermostable mRNA Vaccine against COVID-19. *Cell* **182**, 1271–1283.e16.
- Zohar, T., Loos, C., Fischinger, S., Atyeo, C., Wang, C., Slein, M.D., Burke, J., Yu, J., Feldman, J., Hauser, B.M., et al. (2020). Compromised Humoral Functional Evolution Tracks with SARS-CoV-2 Mortality. *Cell* **183**, 1508–1519.e12.

STAR★METHODS

KEY RESOURCES TABLE

REAGENT or RESOURCE	SOURCE	IDENTIFIER
Antibodies		
UCHT1 (BUV395) [Human anti-CD3]	BD Biosciences	Cat#563546 ; Lot:9058566 ; RRID:AB_2744387
UCHT1 (BUV496) [Human anti-CD3]	BD Biosciences	Cat#612941 ; Lot:1022424 ; RRID:AB_2870222
L200 (BV711) [Human anti-CD4]	BD Biosciences	Cat#563913 ; Lot:03000025 ; RRID:AB_2738484
SK3 (BB630) [Human anti-CD4]	BD Biosciences	Cat#624294 CUSTOM ; Lot:0289566
RPA-T8 (BV570) [Human anti-CD8]	Biolegend	Cat#301037 ; Lot:B281322 ; RRID:AB_10933259
M5E2 (BUV805) [Human anti-CD14]	BD Biosciences	Cat#612902 ; Lot:0262150 ; RRID:AB_2870189
M5E2 (BV480) [Human anti-CD14]	BD Biosciences	Cat#746304 ; Lot: 9133961 ; RRID:AB_2743629
3G8 (BV650) [Human anti-CD16]	Biolegend	Cat#302042 ; Lot:B323847 ; RRID:AB_2563801
HIB19 (APC-eFluor780) [Human anti-CD19]	Thermo Fisher Scientific	Cat#47-0199 ; Lot:2145095 ; RRID:AB_1582231
HIB19 (BV480) [Human anti-CD19]	BD Biosciences	Cat#746457 ; Lot:1021649 ; RRID:AB_2743759
HI100 (PerCP Cy5.5) [Human anti-CD45RA]	BD Biosciences	Cat#563429 ; Lot:8332746 ; RRID:AB_2738199
NCAM16.2 (BUV737) [Human anti-CD56]	BD Biosciences	Cat#564448 ; Lot:8288818 ; RRID:AB_2744432
FN50 (PerCP-eFluor710) [Human anti-CD69]	Thermo Fisher Scientific	Cat#46-0699-42 ; Lot:1920361 ; RRID:AB_2573694
FN50 (BV650) [Human anti-CD69]	Biolegend	Cat# 310934 ; Lot:B303462 ; RRID:AB_2563158
H4A3 (BV786) [Human anti-CD107A]	BD Biosciences	Cat#563869 ; Lot:8144866 ; RRID:AB_2738458
ACT35 (APC) [Human anti-CD134 (OX40)]	BD Biosciences	Cat#563473 ; Lot:1015537 ; RRID:AB_2738230
4B4-1 (PE-Dazzle 594) [Human anti-CD137 (4-1BB)]	Biolegend	Cat# 309826 ; Lot:B253152 ; RRID:AB_2566260
TRAP1 (BV421) [Human anti-CD154 (CD40L)]	BD Biosciences	Cat#563886 ; Lot:9037850 ; RRID:AB_2738466
TRAP1 (PE) [Human anti-CD154 (CD40L)]	BD Biosciences	Cat#555700 ; Lot:7086896 ; RRID:AB_396050
J25D4 (BV421) [Human anti-CD185 (CXCR5)]	Biolegend	Cat# 356920 ; Lot:B325837 ; RRID:AB_2562303
B27 (PECy7) [Human anti-IFN- γ]	BD Biosciences	Cat#557643 ; Lot:8256597 ; RRID:AB_396760
MQ1-17H12 (PE-Dazzle594) [Human anti-IL-2]	Biolegend	Cat#500344 ; Lot:B2261476 ; RRID:AB_2564091
JES3-9D7 (PE) [Human anti-IL-10]	BD Biosciences	Cat#554498 ; Lot:8198773 ; RRID:AB_395434
eBio64CAP17 (eFluor660) [Human anti-IL-17A]	Thermo Fisher Scientific	Cat#50-7179-42 ; Lot:2151998 ; RRID:AB_11149126
Mab11 (Alexa Fluor 488) [Human anti-TNF- α]	Biolegend	Cat#502915 ; Lot:B285221 ; RRID:AB_493121
LIVE/DEAD Fixable dead cell	Thermo Fisher Scientific	Cat # L34960
LIVE-DEAD Fixable AquaVivid Cell Stain	Thermo Fischer Scientific	Cat# P34957
Mouse monoclonal anti-SARS-CoV-2 Spike (CR3022)	Dr M. Gordon Joyce	RRID:AB_2848080
CV3-25	https://www.biorxiv.org/content/10.1101/2021.03.23.436684v1	N/A
Peroxidase AffiniPure Goat Anti-Human IgA + IgG + IgM (H+L)	Jackson ImmunoResearch	Cat # 109-035-064 ; RRID:AB_2337583
Goat anti-Human IgG Fc Cross-Adsorbed Secondary Antibody, HRP	Invitrogen	Cat # 31413
Peroxidase AffiniPure F(ab') ₂ Fragment Goat Anti-Human Serum IgA, α chain specific	Jackson ImmunoResearch	Cat # 109-036-011 ; RRID: AB_2337592

(Continued on next page)

Continued

REAGENT or RESOURCE	SOURCE	IDENTIFIER
<i>Peroxidase AffiniPure Goat Anti-Human IgM, Fc_{5μ} fragment specific</i>	Jackson ImmunoResearch	Cat # 109-035-129; RRID:AB_2337588
<i>Alexa Fluor® 647 AffiniPure Goat Anti-Human IgA + IgG + IgM (H+L)</i>	Jackson ImmunoResearch	Cat # 109-605-064; RRID:AB_2337886
Cell Proliferation Dye eFluor™ 670	Thermo Fisher Scientific	Cat # 65-0840-85
Cell proliferation dye eFluor450	Thermo Fisher Scientific	Cat # 65-0842-85
Biological samples		
SARS-CoV-2 naive donor blood samples	This paper	N/A
SARS-CoV-2 prior infection donor blood samples	This paper	N/A
Chemicals, peptides, and recombinant proteins		
Dulbecco's Modified Eagle's medium (DMEM)	Wisent	Cat# 319-005-CL
Roswell Park Memorial Institute (RPMI)	Thermo Fischer Scientific	Cat# 61870036
Penicillin/Streptomycin	Wisent	Cat# 450-201-EL
Fetal Bovine Serum (FBS)	VWR	Cat# 97068-085
Bovine Serum Albumin (BSA)	Sigma	Cat# A7638
Phosphate Buffered Saline (PBS)	ThermoFischer Scientific	Cat# 10010023
Tween 20	Sigma	Cat# P9416-100ML
Puromycin Dihydrochloride	Millipore Sigma	Cat# P8833
Passive Lysis Buffer	Promega	Cat# E1941
Freestyle 293F expression medium	Thermo Fischer Scientific	Cat# A14525
D-Luciferin Potassium Salt	Thermo Fischer Scientific	Cat# L2916
Formaldehyde 37%	Thermo Fischer Scientific	Cat# F79-500
QuikChange II XL Site-Directed Mutagenesis Kit	Agilent	Cat# 200521
ExpiFectamine 293 transfection reagent	ThermoFisher Scientific	Cat# A14525
Western Lightning Plus-ECL, Enhanced Chemiluminescence Substrate	Perkin Elmer Life Sciences	Cat# NEL105001EA
Ni-NTA agarose	Invitrogen	Invitrogen
PepMix™ SARS-CoV-2 (Spike Glycoprotein)	JPT	Cat#PM-WCPV-S-1
Staphylococcal Enterotoxin B (SEB)	Toxin technology	Cat#BT202
Experimental models: Cell lines		
HEK293T cells	ATCC	Cat# CRL-3216; RRID: CVCL_0063
293T-ACE2 cells	(Prévost et al., 2020)	N/A
FreeStyle 293F cells	ThermoFischer Scientific	Cat# R79007; RRID: CVCL_D603
CEM.NKr CCR5+ cells	NIH AIDS reagent program	Cat# ARP-4376
CEM.NKr CCR5+.S cells	(Anand et al., 2021b)	N/A
HOS cells	ATCC	Cat# CRL-1543
HOS.S cells	(Anand et al., 2021b)	N/A
Recombinant DNA		
pNL4.3 R-E- Luc	NIH AIDS reagent program	Cat# 3418
pcDNA3.1(+)-SARS-CoV-2 RBD	(Beaudoin-Bussièeres et al., 2020)	N/A
pCG1-SARS-CoV-2 Spike D614G	(Beaudoin-Bussièeres et al., 2020)	N/A
pCG1-SARS-CoV-1 Spike	(Hoffmann et al., 2013)	N/A
pCAGGS-OC43 Spike	(Prévost et al., 2020)	N/A
MERS-CoV Spike	(Park et al., 2016)	N/A
pCMV3-HCoV-HKU1 Spike	Sino Biological	Cat# VG40021-UT
pcDNA3.1 SARS-CoV-2 Spike B.1.1.7	Genscript	N/A
pCG1-SARS-CoV-2 Spike D614G/E484K	This paper	N/A
pCG1-SARS-CoV-2 Spike D614G/N501Y	This paper	N/A

(Continued on next page)

Continued

REAGENT or RESOURCE	SOURCE	IDENTIFIER
pCG1-SARS-CoV-2 Spike D614G/N501S	This paper	N/A
pCG1-SARS-CoV-2 Spike D614G/S477N	This paper	N/A
Software and algorithms		
Flow Jo v10.7.1	Flow Jo	https://www.flowjo.com
GraphPad Prism v8.4.3	GraphPad	https://www.graphpad.com
R studio v	R studio	https://rstudio.com
Microsoft Excel v16	Microsoft Office	https://www.microsoft.com/en-ca/microsoft-365/excel
Others		
BD LSRII Flow Cytometer	BD Biosciences	N/A
Symphony cytometer	BD Biosciences	N/A
TriStar LB942 Microplate Reader	Berthold Technologies	N/A

RESOURCE AVAILABILITY

Lead contact

Further information and requests for resources and reagents should be directed to and will be fulfilled by the lead contact, Andrés Finzi (andres.finzi@umontreal.ca)

Materials availability

All unique reagents generated during this study are available from the Lead contact without restriction.

Data and code availability

The published article includes all datasets generated and analyzed for this study. Further information and requests for resources and reagents should be directed to and will be fulfilled by the Lead Contact Author (andres.finzi@umontreal.ca).

EXPERIMENTAL MODEL AND SUBJECT DETAILS

Ethics statement

This study was approved by the CRCHUM ethic committee in accordance with the Declaration of Helsinki (IRB protocol 19.381). Blood samples were obtained from donors who consented to participate in this research project at CHUM (IRB protocol 19.381). Plasma and PBMCs were isolated by centrifugation and Ficoll gradient, and samples stored at -80°C and in liquid nitrogen, respectively, until use.

Human subjects

No specific criteria such as number of patients (sample size), clinical or demographic were used for inclusion, beyond PCR confirmed SARS-CoV-2 infection in adults. Information related to their average age and gender is reported in [Table 1](#).

Plasma and antibodies

Plasma from SARS-CoV-2 naive and PI donors were collected, heat-inactivated for 1 h at 56°C and stored at -80°C until ready to use in subsequent experiments. Plasma from uninfected donors collected before the pandemic were used as negative controls and used to calculate the seropositivity threshold in our ELISA, cell-based ELISA, ADCC and flow cytometry assays (see below). The RBD-specific monoclonal antibody CR3022 was used as a positive control in our ELISA, cell-based ELISA, and flow cytometry assays and was previously described ([Anand et al., 2021a](#); [Beaudoin-Bussi eres et al., 2020](#); [Pr evost et al., 2020](#)). Horseradish peroxidase (HRP)-conjugated Abs able to detect all Ig isotypes (anti-human IgM+IgG+IgA; Jackson ImmunoResearch Laboratories) or specific for the Fc region of human IgG (Invitrogen), the Fc region of human IgM (Jackson ImmunoResearch Laboratories) or the Fc region of human IgA (Jackson ImmunoResearch Laboratories) were used as secondary Abs to detect Ab binding in ELISA and cell-based ELISA experiments. Alexa Fluor-647-conjugated goat anti-human Abs able to detect all Ig isotypes (anti-human IgM+IgG+IgA; Jackson ImmunoResearch Laboratories) were used as secondary Ab to detect plasma binding in flow cytometry experiments.

Cell lines

293T human embryonic kidney cells (obtained from ATCC) were maintained at 37°C under 5% CO_2 in Dulbecco's modified Eagle's medium (DMEM) (Wisent) containing 5% fetal bovine serum (FBS) (VWR) and 100 $\mu\text{g}/\text{mL}$ of penicillin-streptomycin (Wisent). CEM.NKr CCR5+ cells (NIH AIDS reagent program) were maintained at 37°C under 5% CO_2 in Roswell Park Memorial Institute

(RPMI) 1640 medium (GIBCO) containing 10% FBS and 100 $\mu\text{g}/\text{mL}$ of penicillin-streptomycin. The 293T-ACE2 cell line was previously reported (Prévost et al., 2020). HOS and CEM.NKr CCR5+ cells stably expressing the SARS-CoV-2 S glycoproteins were previously reported (Anand et al., 2021b).

METHOD DETAILS

Plasmids

The plasmids expressing the human coronavirus S of SARS-CoV-2, SARS-CoV-1 (Hoffmann et al., 2013, 2020), HCoV-OC43 (Prévost et al., 2020) and MERS-CoV (Park et al., 2016) or the SARS-CoV-2 S RBD (Beaudoin-Bussi eres et al., 2020) were previously reported. The HCoV-HKU1 S expressing plasmid was purchased from Sino Biological. SARS-CoV-2 S mutations were introduced using the QuikChange II XL site-directed mutagenesis protocol (Stratagene). The presence of the desired mutations was determined by automated DNA sequencing. The plasmid encoding the S of the B.1.1.7 variant was codon-optimized and synthesized by Genscript.

Protein expression and purification

FreeStyle 293F cells (Invitrogen) were grown in FreeStyle 293F medium (Invitrogen) to a density of 1×10^6 cells/mL at 37°C with 8% CO₂ with regular agitation (150 rpm). Cells were transfected with a plasmid coding for SARS-CoV-2 S RBD using ExpiFectamine 293 transfection reagent, as directed by the manufacturer (Invitrogen). One week later, cells were pelleted and discarded. Supernatants were filtered using a 0.22 μm filter (Thermo Fisher Scientific). The recombinant RBD proteins were purified by nickel affinity columns, as directed by the manufacturer (Invitrogen). The RBD preparations were dialyzed against phosphate-buffered saline (PBS) and stored in aliquots at -80°C until further use. To assess purity, recombinant proteins were loaded on SDS-PAGE gels and stained with Coomassie Blue.

Enzyme-linked immunosorbent assay (ELISA)

The SARS-CoV-2 RBD ELISA assay used was previously described (Beaudoin-Bussi eres et al., 2020; Prévost et al., 2020). Briefly, recombinant SARS-CoV-2 S RBD proteins (2.5 $\mu\text{g}/\text{mL}$), or bovine serum albumin (BSA) (2.5 $\mu\text{g}/\text{mL}$) as a negative control, were prepared in PBS and were adsorbed to plates (MaxiSorp Nunc) overnight at 4°C. Coated wells were subsequently blocked with blocking buffer (Tris-buffered saline [TBS] containing 0.1% Tween20 and 2% BSA) for 1 h at room temperature. Wells were then washed four times with washing buffer (Tris-buffered saline [TBS] containing 0.1% Tween20). CR3022 mAb (50 ng/mL) or a 1/250 dilution of plasma from SARS-CoV-2-naive or PI donors were prepared in a diluted solution of blocking buffer (0.1% BSA) and incubated with the RBD-coated wells for 90 min at room temperature. Plates were washed four times with washing buffer followed by incubation with secondary Abs (diluted in a diluted solution of blocking buffer (0.4% BSA)) for 1 h at room temperature, followed by four washes. HRP enzyme activity was determined after the addition of a 1:1 mix of Western Lightning oxidizing and luminol reagents (Perkin Elmer Life Sciences). Light emission was measured with a LB942 TriStar luminometer (Berthold Technologies). Signal obtained with BSA was subtracted for each plasma and was then normalized to the signal obtained with CR3022 present in each plate. The seropositivity threshold was established using the following formula: mean of all SARS-CoV-2 negative plasma + (3 standard deviation of the mean of all SARS-CoV-2 negative plasma).

Cell-based ELISA

Detection of the trimeric SARS-CoV-2 S at the surface of HOS cells was performed by a previously-described cell-based enzyme-linked immunosorbent assay (ELISA) (Anand et al., 2021b). Briefly, parental HOS cells or HOS-S cells were seeded in 96-well plates (4×10^4 cells per well) overnight. Cells were blocked with blocking buffer (10 mg/mL nonfat dry milk, 1.8 mM CaCl₂, 1 mM MgCl₂, 25 mM Tris [pH 7.5], and 140 mM NaCl) for 30 min. CR3022 mAb (1 $\mu\text{g}/\text{mL}$) or plasma from SARS-CoV-2 naive or PI donors (at a dilution of 1/250) were prepared in blocking buffer and incubated with the cells for 1 h at room temperature. Respective HRP-conjugated Abs were then incubated with the samples for 45 min at room temperature. For all conditions, cells were washed 6 times with blocking buffer and 6 times with washing buffer (1.8 mM CaCl₂, 1 mM MgCl₂, 25 mM Tris [pH 7.5], and 140 mM NaCl). HRP enzyme activity was determined after the addition of a 1:1 mix of Western Lightning oxidizing and luminol reagents (PerkinElmer Life Sciences). Light emission was measured with an LB942 TriStar luminometer (Berthold Technologies). Signal obtained with parental HOS was subtracted for each plasma and was then normalized to the signal obtained with CR3022 mAb present in each plate. The seropositivity threshold was established using the following formula: mean of all SARS-CoV-2 negative plasma + (3 standard deviation of the mean of all SARS-CoV-2 negative plasma).

Cell surface staining and flow cytometry analysis

293T cells were transfected with full length S of different *Betacoronavirus*. 48 h post-transfection, S-expressing cells were stained with the CV3-25 Ab or plasma from SARS-CoV-2-naive or PI donors, prior and after vaccination (1/250 dilution). AlexaFluor-647-conjugated goat anti-human IgM+IgG+IgA Abs (1/800 dilution) were used as secondary Abs. The percentage of transduced cells (GFP+ cells) was determined by gating the living cell population based on viability dye staining (Aqua Vivid, Invitrogen). Samples were acquired on a LSRII cytometer (BD Biosciences) and data analysis was performed using FlowJo v10.7.1 (Tree Star). The seropositivity threshold was established using the following formula: (mean of all SARS-CoV-2 negative plasma + (3 standard deviation of the mean of all SARS-CoV-2 negative plasma)).

ADCC assay

For evaluation of anti-SARS-CoV-2 antibody-dependent cellular cytotoxicity (ADCC), parental CEM.NKr CCR5+ cells were mixed at a 1:1 ratio with CEM.NKr.SARS-CoV-2.S cells. These cells were stained for viability (AquaVivid; Thermo Fisher Scientific, Waltham, MA, USA) and cellular dyes (cell proliferation dye eFluor670; Thermo Fisher Scientific) to be used as target cells. Overnight rested PBMCs were stained with another cellular marker (cell proliferation dye eFluor450; Thermo Fisher Scientific) and used as effector cells. Stained target and effector cells were mixed at a ratio of 1:10 in 96-well V-bottom plates. Plasma from SARS-CoV-2 naive or PI individuals (1/500 dilution) or monoclonal antibody CR3022 (1 μ g/mL) were added to the appropriate wells. The plates were subsequently centrifuged for 1 min at 300 g, and incubated at 37°C, 5% CO₂ for 5 h before being fixed in a 2% PBS-formaldehyde solution. ADCC activity was calculated using the formula: $[(\% \text{ of GFP}^+ \text{ cells in Targets plus Effectors}) - (\% \text{ of GFP}^+ \text{ cells in Targets plus Effectors plus plasma/antibody})] / (\% \text{ of GFP}^+ \text{ cells in Targets}) \times 100$ by gating on transduced live target cells. All samples were acquired on an LSRII cytometer (BD Biosciences) and data analysis was performed using FlowJo v10.7.1 (Tree Star). The specificity threshold was established using the following formula: (mean of all SARS-CoV-2 negative plasma + (3 standard deviation of the mean of all SARS-CoV-2 negative plasma)).

Viral infectivity

293T cells were transfected with the lentiviral vector pNL4.3 R-E- Luc (NIH AIDS Reagent Program) and plasmid encoding for the indicated S glycoprotein (D614G, B.1.1.7, D614G/E484K, D614G/N501S, D614G/S477N and D614G/N501Y) at a ratio of 5:4. Two days post-transfection, cell supernatants were harvested and stored at -80°C until use. The RT activity was evaluated by measure of the incorporation of [*methy*-³H]TTP into cDNA of a poly(rA) template in the presence of virion-associated RT and oligo(dT). Normalized amount of RT activity pseudoviral particles were added to 293T-ACE2 target cells for 48 h at 37°C. Then, cells were lysed by the addition of 30 μ L of passive lysis buffer (Promega) followed by one freeze-thaw cycle. An LB942 TriStar luminometer (Berthold Technologies) was used to measure the luciferase activity of each well after the addition of 100 μ L of luciferin buffer (15mM MgSO₄, 15mM KPO₄ [pH 7.8], 1mM ATP, and 1mM dithiothreitol) and 50 μ L of 1mM d-luciferin potassium salt (Thermo Fisher Scientific). RLU values obtained were normalized to D614G.

Virus neutralization assay

293T cells were transfected with the lentiviral vector pNL4.3 R-E- Luc (NIH AIDS Reagent Program) and a plasmid encoding for the indicated S glycoprotein (D614G, B.1.1.7, D614G/E484K, D614G/N501S, D614G/S477N, D614G/N501Y and SARS-CoV-1) at a ratio of 5:4. Two days post-transfection, cell supernatants were harvested and stored at -80°C until use. 293T-ACE2 target cells were seeded at a density of 1×10^4 cells/well in 96-well luminometer-compatible tissue culture plates (Perkin Elmer) 24 h before infection. Pseudoviral particles were incubated with the indicated plasma dilutions (1/50; 1/250; 1/1250; 1/6250; 1/31250) for 1 h at 37°C and were then added to the target cells followed by incubation for 48 h at 37°C. Then, cells were lysed by the addition of 30 μ L of passive lysis buffer (Promega) followed by one freeze-thaw cycle. An LB942 TriStar luminometer (Berthold Technologies) was used to measure the luciferase activity of each well after the addition of 100 μ L of luciferin buffer (15mM MgSO₄, 15mM KPO₄ [pH 7.8], 1mM ATP, and 1mM dithiothreitol) and 50 μ L of 1mM d-luciferin potassium salt (Thermo Fisher Scientific). The neutralization half-maximal inhibitory dilution (ID₅₀) represents the plasma dilution to inhibit 50% of the infection of 293T-ACE2 cells by SARS-CoV-2 pseudoviruses.

Intracellular cytokine staining

PBMCs were thawed and rested for 2h in RPMI 1640 medium supplemented with 10% FBS, Penicillin-Streptomycin (Thermo Fisher scientific, Waltham, MA) and HEPES (Thermo Fisher scientific, Waltham, MA). 2×10^6 PBMCs were stimulated with a S glycoprotein peptide pool (0.5 μ g/mL per peptide from JPT, Berlin, Germany) corresponding to the pool of 315 overlapping peptides (15-mers) spanning the complete amino acid sequence of the S glycoprotein.

Cell stimulation was carried out for 6 h in the presence of mouse anti-human CD107A, Brefeldin A and monensin (BD Biosciences, San Jose, CA) at 37°C and 5% CO₂. DMSO-treated cells served as a negative control. Cells were stained for aquavivid viability marker (Thermo Fisher scientific, Waltham, MA) for 20cmin at 4°C and surface markers (30cmin, 4°C), followed by intracellular detection of cytokines using the IC Fixation/Permeabilization kit (Thermo Fisher scientific, Waltham, MA) according to the manufacturer's protocol before acquisition on a Symphony flow cytometer (BD Biosciences, San Jose, CA). Abs used are listed in the [Table S2](#). Stained PBMCs were acquired on Symphony cytometer (BD Biosciences) and analyzed using FlowJo v10.7.1 software.

Activation-induced marker assay

PBMCs were thawed and rested for 3 h in 96-well flat-bottom plates in RPMI 1640 supplemented with HEPES, penicillin and streptomycin and 10% FBS. 1.7×10^6 PBMCs were stimulated with a S glycoprotein peptide pool (0.5 μ g/mL per peptide) for 15 h at 37°C and 5% CO₂. A DMSO-treated condition served as a negative control and SEB-treated condition (0.5 μ g/mL) as positive control. Cells were stained for viability dye for 20 min at 4°C then surface markers (30cmin, 4°C) (See [Table S3](#) for Ab staining panel). Cells were fixed using 2% paraformaldehyde before acquisition on Symphony cytometer (BD Biosciences). Analyses were performed using FlowJo v10.7.1 software.

QUANTIFICATION AND STATISTICAL ANALYSIS

Statistical analysis

Symbols represent biologically independent samples from SARS-CoV-2 naive individuals ($n = 24$) and SARS-CoV-2 PI individuals ($n = 24$). Lines connect data from the same donor. Statistics were analyzed using GraphPad Prism version 8.0.1 (GraphPad, San Diego, CA). Every dataset was tested for statistical normality and this information was used to apply the appropriate (parametric or nonparametric) statistical test. Differences in responses for the same patient before and after vaccination were performed using Wilcoxon matched pair tests. Differences in responses between naive and PI individuals were measured by Mann-Whitney tests. Differences in responses against the SARS-CoV-2 variants for the same patient were measured by Friedman test. P values < 0.05 were considered significant; significance values are indicated as * $p < 0.05$, ** $p < 0.01$, *** $p < 0.001$, **** $p < 0.0001$. Line charts were created with Prism 8.4.3 using normalized data and Akima spline interpolation. For correlations, Spearman's R correlation coefficient was applied. Statistical tests were two-sided and $p < 0.05$ was considered significant.

Software scripts and visualization

Normalized heatmaps were generated using the `complexheatmap`, `tidyverse`, and `viridis` packages in R and RStudio (R; RStudio). Normalizations were done per "Analysis group," e.g., separately for all neutralization data, T cell responses, etc, except for binding analysis, which was normalized per individual parameter because different Abs are needed for the detection of Ig responses. IDs were grouped and clustered separately according to naive versus PI individuals, and also according to the time points before vaccination (V0) and after vaccination (V1). Squared correlograms were generated using the `corrplot` and `RColorBrewer` packages in program R and RStudio. Edge bundling graphs were generated in undirected mode in R and RStudio using `ggraph`, `igraph`, `tidyverse`, and `RColorBrewer` packages. Edges are only shown if $p < 0.05$, and nodes are sized according to the connecting edges' r values. Nodes are color-coded according to groups of parameters. Area graphs were generated for the display of normalized time series. The plots were created in RawGraphs using `DensityDesign` interpolation and vertically un-centered values (Mauri et al., 2017). Line charts in overlay were created with Prism 8.4.3 using normalized data per response and Akima spline interpolation.